Technical Report Documentation Page

1. Report No. FHWA/TX-02/4177-2	2. Government Accession No.	3. Recipient's Catalog No.
4. Title and Subtitle RECYCLED ASPHALT PAVEMENT AND CRUSHED CONCRETE BACKFILL: RESULTS FROM INITIAL DURABILITY AND GEOTECHNICAL TESTS		5. Date October 2002
7. Author(s) Ellen M. Rathje, Alan F. Rauch, Kevin J. Folliard, David Trejo, Dallas Little, Chirayus Viyanant, Moses Ogalla, Michael Esfeller		6. Performing Organization Code 8. Performing Organization Report No. 4177-2
9. Performing Organization Name and Address Center for Transportation Research The University of Texas at Austin 3208 Red River, Suite 200 Austin, TX 78705-2650		10. Work Unit No. (TRAIS) 11. Contract or Grant No. 0-4177
12. Sponsoring Agency Name and Address Texas Department of Transportation Research and Technology Implementation Office P.O. Box 5080 Austin, TX 78763-5080		13. Type of Report and Period Covered Research Report, 1 Sept 2001 – 1 Sept 2002 14. Sponsoring Agency Code

15. Supplementary Notes
Project conducted in cooperation with the Texas Department of Transportation, U.S. Department of Transportation, Federal Highway Administration.

16. Abstract

This report describes research results from the second year of a three-year study focused on the use of recycled asphalt pavement (RAP) and crushed concrete (CC) as backfill for mechanically stabilized earth (MSE) walls. The objectives of the research project are reviewed. The compaction characteristics of RAP and CC are presented, and the effect of compaction on particle breakdown is discussed. Tests to evaluate the accuracy of nuclear gauges, when used to measure the compacted density and water content of RAP and CC in the field, are also discussed. Results indicate that the nuclear gauge overpredicts the as-compacted moist density and water content of RAP and CC. Triaxial strength testing of RAP and CC are presented, and indicate that these materials exhibit adequate strength for MSE wall applications. Results are presented from expansion tests performed on various CC specimens to evaluate the potential for excessive heave or expansion after compaction. Expansion appears only to be a problem when the CC contains significant sulfates, but the sulfate levels necessary to cause problems are not expected to occur in the field. Preliminary results from corrosion tests indicate that RAP and CC do not adversely affect the corrosion rate of metallic strip reinforcement at early exposure periods.

17. Key Words Recycled asphalt, crushed concrete, MSE walls	18. Distribution Statement No restrictions. This document is available to the public through the National Technical Information Service, Springfield, Virginia 22161.

19. Security Classif. (of report) Unclassified	20. Security Classif. (of this page) Unclassified	21. No. of pages 84	22. Price

Form DOT F 1700.7 (8-72) Reproduction of completed page authorized

Recycled Asphalt Pavement and Crushed Concrete Backfill: Results from Initial Durability and Geotechnical Tests

The University of Texas at Austin
Ellen M. Rathje
Alan F. Rauch
Kevin J. Folliard
Chirayus Viyanant
Moses Ogalla

Texas A&M University
David Trejo
Dallas Little
Michael Esfeller

Research Report 4177-2

Research Project 0-4177
Use of Recycled Asphalt Pavement and Crushed Concrete as Backfill for Mechanically Stabilized Earth Retaining Walls

Conducted for the
Texas Department Of Transportation
in cooperation with the
U.S. Department of Transportation
Federal Highway Administration
by the
Center for Transportation Research
Bureau of Engineering Research
The University of Texas at Austin

October 2002

Disclaimers

The contents of this report reflect the views of the authors, who are responsible for the facts and the accuracy of the data presented herein. The contents do not necessarily reflect the official views or policies of the Federal Highway Administration or the Texas Department of Transportation. This report does not constitute a standard, specification, or regulation.

There was no invention or discovery conceived or first actually reduced to practice in the course of or under this contract, including any art, method, process, machine, manufacture, design or composition of matter, or any new and useful improvement thereof, or any variety of plant, which is or may be patentable under the patent laws of the United States of America or any foreign country.

NOT INTENDED FOR CONSTRUCTION,
BIDDING, OR PERMIT PURPOSES

Ellen M. Rathje, Ph.D.
Research Supervisor

Acknowledgments

The support and assistance of the personnel at the Texas Department of Transportation are gratefully acknowledged. These personnel include the project coordinator Ronald Medlock (BRG), the project advisor Mark McClelland (BRG), the project director Marcus Galvan (BRG), and the project monitoring committee, which includes John Delphia (BRY), Harold Albers (CST), and Mario Garza (CRP).

Research performed in cooperation with the Texas Department of Transportation and the U.S. Department of Transportation, Federal Highway Administration.

Table of Contents

1. Introduction 1

2. Preliminary Results from Geotechnical Testing 5

2.1 Index and Compaction Properties 5

2.1.1 Specific Gravity 5

2.1.2 Grain Size Distribution 7

2.1.3 Laboratory Compaction Characteristics 8

2.1.4 Degradation of Materials after Compaction 8

2.2 Field Compaction Control 10

2.2.1 Field Density Measurement Methods 11

2.2.2 Field Testing Program 15

2.2.3 Test Results and Discussion 18

2.2.4 Conclusions from Field Compaction Control Tests 25

2.3 Preliminary Results from Triaxial Tests 26

2.3.1 Specimen Preparation and Testing Program 26

2.3.2 Hydraulic Conductivity 27

2.3.3 Drained Shear Strength 28

2.4 Design and Construction of the Large Direct Shear Machine 32

3. Durability of Crushed Concrete 37

3.1 Background 37

3.2 ASR Testing Using Crushed Concrete 40

3.2.1 Concrete Prism Test (Modified ASTM C 1293) 42

3.2.2 Expansion Testing of Laboratory CC 44

3.2.3 Experimental Results and Discussions 46

3.2.4 Expansion Testing of Commercial CC 47

3.3 Sulfate Attack Testing Using Crushed Concrete 48

3.3.1 Accelerated Sulfate Expansion Tests 50

3.3.2 Expansion Testing of Laboratory CC 50

3.3.3 Experimental Results and Discussions 53

3.3.4 Sulfate Attack Testing of Commercial CC 54

3.4 Summary 55

4. Preliminary Results from Corrosion Studies 57

4.1 Materials 57

4.1.1 Aggregate 57
4.1.2 Reinforcement 58
4.2 Experimental Design and Test Procedures 59
4.2.1 Short-Term Test Procedures 59
4.2.2 Long-Term Test Procedures 59
4.3 Preliminary Results and Discussion 61
4.4 Summary 64
5. Summary 65
References 67

List of Figures

Figure 2.1 Grain size distribution of testing materials from actual stockpiles. 6
Figure 2.2 Moisture-density relationship for the three test materials (Tex-113-E test method). 7
Figure 2.3 Degradation of materials after compaction using the Tex-113-E method. 9
Figure 2.4 Nuclear test gauge for control of compaction in an MSE wall backfill. 11
Figure 2.5 Nuclear gauge setup for the (a) direct transmission method and (b) backscatter method (from Troxler 2001). 13
Figure 2.6 Testing on the three material stockpiles. 15
Figure 2.7 Conventional fill material (CFM) stockpile and test locations. 16
Figure 2.8 Figure 2.8. Crushed Concrete (CC) stockpile and test locations. 16
Figure 2.9 Recycled asphalt pavement (RAP) stockpile and test locations. 17
Figure 2.10 Nuclear gauge tests. 18
Figure 2.11 Excavation of hole for rubber balloon test. 19
Figure 2.12 Rubber balloon test of material density. 19
Figure 2.13 Comparison of moist densities measured by rubber balloon and nuclear gauge methods in all three materials. 20
Figure 2.14 Comparison of moist density of RAP measured by rubber balloon and test pit methods. 23
Figure 2.15 Comparison of the moisture contents measured with the nuclear gauge and oven drying. 24
Figure 2.16 Grain size distribution of reference material and triaxial test specimens. 26
Figure 2.17 Results from consolidated drained triaxial tests on the test materials. 29
Figure 2.18 Three-dimensional, schematic drawing of the large direct shear test machine (courtesy of Hi-Tech Products, Inc.) 33
Figure 2.19 Vertical cross-section of the large-scale direct shear test machine. 34
Figure 3.1 Expansion of Prisms 1 to 18, Exposed to Alkali Solution for 42 days, Stored in 60 °C Control Chamber 43
Figure 3.2 Expansion of Prisms 19 to 33, Moist Cured for 42 days at 23 °C. 43
Figure 3.3 Test Apparatus for Compacted CC Expansion Samples 44
Figure 3.4 Compacted CC ASR Expansion Samples, Stored in 38°C Reaction Chamber. Samples 1,2,3 in Water; samples 4,5,6 in 1N-NaOH

Solution (Samples 1-6 Prepared from Prisms 1 to 18, which that had Previously Experienced ASR Attack) 45

Figure 3.5 Compacted CC ASR Expansion Samples, Stored in 38 °C Reaction Chamber. Samples 7,8,9 in Water; Samples 10,11,12 in 1N-NaOH Solution (Samples 7-12 Prepared from Prisms 19 to 33 that had not Experienced ASR Attack) 46

Figure 3.6 Compacted Commercial CC ASR Expansion Samples, Stored in 38 °C Reaction Chamber, in 1N-NaOH Solution 48

Figure 3.7 Expansion Prisms 1 to 18, Exposed to Sulfate Solution for 30 days, Stored in 38 °C Control Chamber 51

Figure 3.8 Expansion Prisms 19 to 36, Exposed to Saturated Lime Solution for 30 days, Stored in 38 °C Control Chamber 52

Figure 3.9 Compacted CC Sulfate Expansion Results, 38 °C Reaction Chamber. Samples 1,2,3 in Water; Samples 4,5,6 in 5% Sulfate Solution (Samples 1-6 Prepared from Prisms 1 to 18 that had Previously Experience Sulfate Attack) 53

Figure 3.10 Compacted Commercial CC Sulfate Expansion, 38 °C Reaction Chamber, in 5% Sulfate Solution 54

Figure 4.1 Short-term testing diagram. 59

Figure 4.2 Long-term testing diagram. 60

Figure 4.3 Front and sectional side view of long-term test samples equipped for polarization resistance testing. 60

Figure 4.4 Boxplot of average corrosion rates for each group over 64 days. 62

Figure 4.5 Boxplot of average potential readings for each group over 64 days. 64

List of Tables

Table 2.1 Specific gravity of test materials. 6

Table 2.2 Specimen compaction specifications based on Tex-113-E compaction test results. 8

Table 2.3 Minimum and maximum dry densities of each material and relative density when compacted to optimum conditions with the Tex-113-E method. 10

Table 2.4 Ratio of moist densities measured by nuclear gauge ($\gamma_{m,NG}$) and rubber balloon method ($\gamma_{m,BAL}$). 21

Table 2.5 Ratio of moisture contents measured by nuclear gauge (w_{NG}) and oven drying (w_{OVEN}). 24

Table 2.6 Summary of preliminary drained strength properties. 30

Table 3.1 TxDOT and FHWA MSE Wall Backfill Specifications 39

Table 3.2 ASR Concrete Mixture Proportions (per m3 of concrete, w/c=0.45, ACI 211) 41

Table 3.3 Sulfate Concrete Mixture Proportions (per m^3 of concrete) W/C=0.68, ACI 211 49

Table 4.1 Selected sources of CFM, CC, and RAP backfill materials. 57

Table 4.2 Reference gradation for CFM, CC, and RAP backfill materials. 58

1. Introduction

The concept of mechanically stabilized earth (MSE) was introduced in the United States in the 1970s, with the first reinforced earth wall being constructed in southern California in 1972 (Mitchell and Christopher 1990). Since that time, both earth retaining structures and earth embankments incorporating mechanically stabilized earth have been constructed throughout the country. The popularity of mechanically stabilized earth systems can been credited to their low cost, aesthetic appeal, simple construction, and reliability (Mitchell and Christopher 1990). To ensure long-term integrity of the wall, conventional backfills consisting predominantly of granular soils have been recommended and used in the past. This limitation on material type can significantly increase the cost of construction on some projects due to the cost of transporting select material to the construction site.

The Texas Department of Transportation (TxDOT) is a leader in the construction of MSE walls. However, many parts of Texas do not have backfill materials that meet the current TxDOT material specifications for MSE walls. In these cases, contractors are forced to transport select backfill material from other parts of the state. These transportation costs can be significant and may make the construction of MSE walls impractical. At the same time, contractors often must dispose of crushed concrete and asphalt from demolished pavements. Again, contractors must pay transportation costs, as well as disposal fees, to discard these materials. One solution is to recycle these materials, often called recycled asphalt pavement (RAP) and crushed concrete (CC), and use them as alternative backfill. Throughout the United States, substantial amounts of RAP and CC are being produced, and it is estimated that more than 73 million tons of RAP and 95 million tons of CC are being processed each year (Kelly 1998). If RAP and CC were used as backfill for MSE walls, transportation and disposal costs for these materials could be greatly reduced, translating into significant savings for TxDOT.

RAP is removed and/or reprocessed pavement material containing asphalt and aggregates. Asphalt pavement is generally removed either by milling or full-depth removal. Milling involves removal of the pavement surface using a milling machine, which can remove up to 2 inches with a single pass. Full-depth removal is usually achieved with a

pneumatic pavement breaker or a rhino horn on a bulldozer. The broken materials are transferred to a central facility for a series of recycling processes including crushing, screening, conveying, and stacking. Asphalt pavement can also be pulverized in place and incorporated into granular or stabilized base courses using a self-propelled pulverizing machine (FHWA 2000). In-place recycling eliminates the cost of transporting material to and from the processing facility.

CC is generated through the demolition of Portland cement concrete elements from roads, runways, and concrete structures. Crushed concrete is generally removed by a backhoe or payloader and loaded into dump trucks for removal from the site. In cases where crushed concrete is secured from demolished pavements, soil and small quantities of bituminous concrete can be expected in the excavated materials. Usually reclaimed concrete materials are hauled to a central processing plant where crushing, screening, and ferrous metal recovery are performed before stockpiling. However, on-site recycling and processing can be performed with a mobile plant. At a central plant, reclaimed materials are subjected to primary and secondary crushers. The primary crusher breaks the reinforcing elements from the concrete debris and breaks them down into particles 3 to 4 inches in diameter. Removal of reinforcing steel by an electromagnetic separator occurs while conveying the materials to the secondary crusher. The secondary crusher further breaks down the particle sizes to the desired gradation. Stockpiling of crushed concrete is usually done through the separation of coarse and fines particles to avoid inadvertent mixing of materials.

TxDOT Project 0-4177 is evaluating the potential use of RAP and CC as a backfill material in MSE walls. Typical geotechnical tests, reinforcement pullout tests, and corrosion and degradation tests are being performed. The project consists of an extensive laboratory investigation that will fully characterize RAP and CC, and will evaluate the effect of these materials on the corrosion of metallic reinforcements typically used in MSE walls. The results from this investigation will be used to develop appropriate modifications to the materials specifications, laboratory test methods, and other related design and construction issues as needed to permit the use of these materials as backfill for MSE walls.

This report represents a summary of the work performed during Year 2 of this three-year project. Tasks performed are described and preliminary results are presented. The report consists of five chapters. After the introduction presented in Chapter 1, Chapter 2 describes the preliminary results from geotechnical testing. These results include strength data from triaxial compression tests, evaluation of nuclear gauges to measure field density and water content, and description of the large direct shear machine designed and built for shear strength testing of RAP and CC. Chapter 3 discusses the durability of crushed concrete with respect to the deleterious material and impurities that may affect MSE wall performance. Chapter 4 presents preliminary results from corrosion studies. Corrosion is an important issue because CC and RAP can affect the corrosion rate of the steel reinforcement strips within the MSE wall. Excessive corrosion can lead to excessive deformation of the wall or full collapse. A summary and conclusions are presented in Chapter 5.

2. Preliminary Results from Geotechnical Testing

This chapter summarizes preliminary results from tests to characterize the geotechnical properties of RAP and CC backfill materials. Data from tests on a conventional fill material (CFM), consisting of crushed limestone, are included for comparison. Laboratory compaction characteristics and the selection of a reference gradation were discussed in the first annual report for this project (Rathje et al. 2001). These data are reviewed here, together with additional index properties for these materials. Tests to evaluate the accuracy of nuclear gauges, when used to measure the compacted density and water content of RAP and CC in the field, are also discussed. Preliminary strength data from drained triaxial compression tests are presented, along with a description of the large direct shear machine designed and built for testing the full gradation of typical RAP and CC materials.

2.1 Index and Compaction Properties

2.1.1 Specific Gravity

The specific gravity (G_s) of each material is given in Table 2.1. The specific gravity of particles larger than the No. 4 sieve (4.75 mm) was measured using test method ASTM C127, while the G_s of smaller particles was measured using test method ASTM D854. The specific gravity of the composite material was then computed as a weighted average of these values. The test results indicate that the large and small particles have very similar values of G_s. The specific gravity of RAP is significantly smaller than that of CC and CFM, most likely due to the residual bitumen coating the aggregates.

Table 2.1 Specific gravity of test materials.

Material	*Specific Gravity (G_s)*		
	Particles > 4.75 mm	*Particles < 4.75 mm*	*Composite*
CC	2.62	2.62	2.62
RAP	2.36	2.28	2.33
CFM	2.64	2.69	2.66

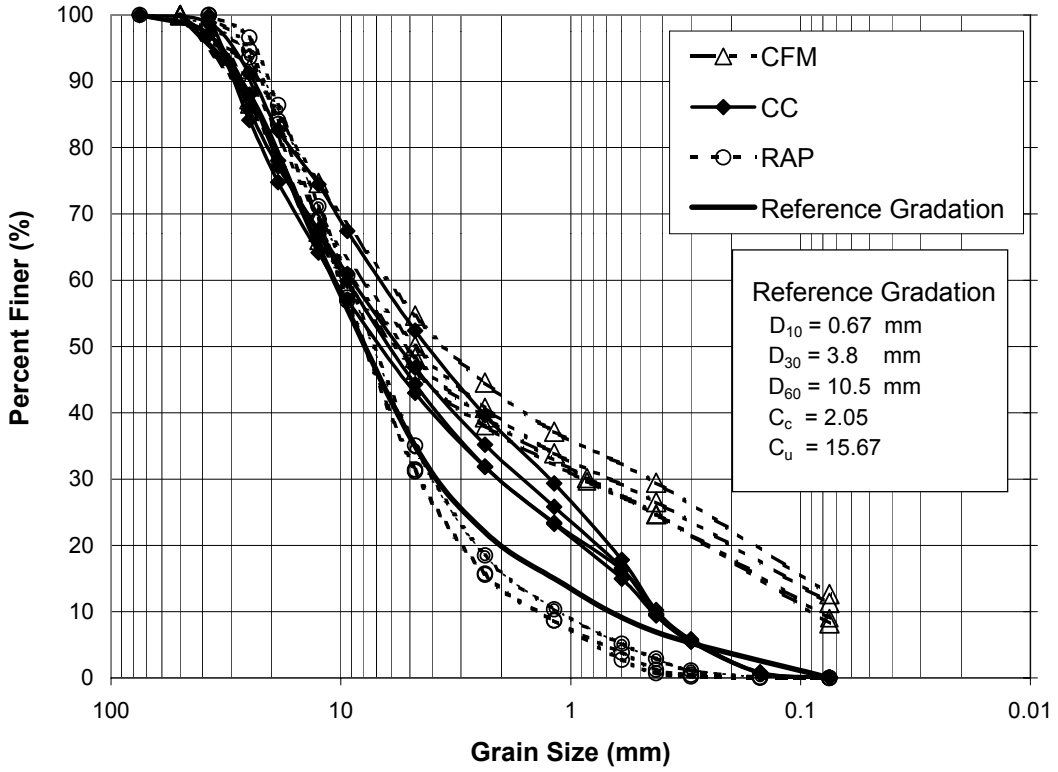

Figure 2.1 Grain size distribution of testing materials from actual stockpiles.

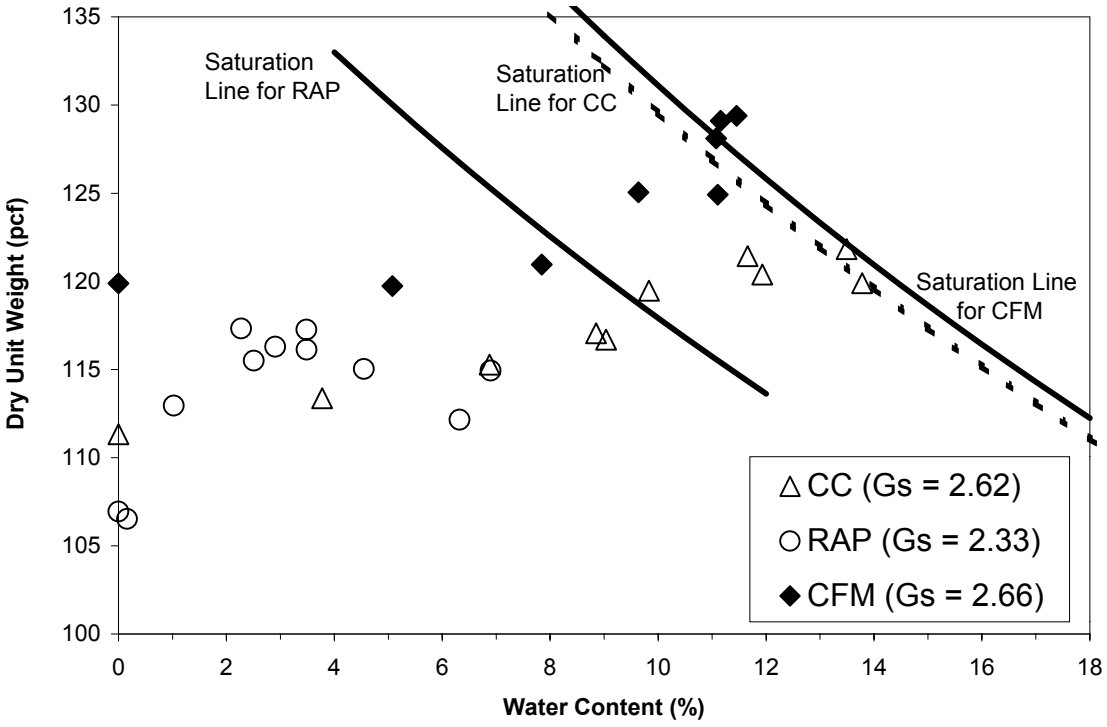

Figure 2.2 Moisture-density relationship for the three test materials (Tex-113-E test method).

2.1.2 Grain Size Distribution

The gradation of each material was determined through sieve tests, conducted in accordance with ASTM D422, using sieves ranging in size from 0.075 to 75 mm (0.0029 to 3 inch). The test data (Figure 2.1) show that the RAP and CC contain less than 1% fines (passing the No. 200 sieve), while the CFM had about 10% fines. Subsequent tests on these materials will be conducted on samples mixed to a selected reference gradation, also shown in Figure 2.1, as discussed in Rathje et al. (2001). Using a single reference gradation eliminates the effect of different grain size distributions on the measured properties, thereby allowing the test results to be interpreted in terms of the composition of the different materials. The reference gradation will be used in preparing specimens throughout the experimental program, except where the maximum particle size is limited by the test equipment.

2.1.3 Laboratory Compaction Characteristics

As discussed in Rathje et al. (2001), compaction characteristics for each material were measured in accordance with the TxDOT Tex-113-E test method. The moisture-density relationship for each material was thus established as shown in Figure 2.2. Similar to other clean gravel materials, the compaction curves do not exhibit a distinct peak. Based on this compaction test data, recommended compaction water contents and the expected dry unit weights for specimen preparation were established as given in Table 2.2.

Table 2.2 Specimen compaction specifications based on Tex-113-E compaction test results.

Material	*Recommended water content (%)*	*Expected dry unit weight (lb/ft^3)*
CC	10	119
RAP	3	117
CFM	10	125

2.1.4 Degradation of Materials after Compaction

Fines content is a major factor in assessing the quality of backfill material. With crushed and recycled materials, additional fines may be created during compaction when larger particles in the material are broken. The degradation of CC, RAP, and CFM due to impact compaction was thus evaluated. Samples of all three materials were mixed to the reference gradation (Figure 2.1) and the recommended water content (Table 2.2). The material was then subjected to impact compaction following the Tex-113-E method. The grain size distribution curves of the test materials before and after compaction are shown in Figure 2.3. Each curve represents the average size distribution of multiple test specimens. Based on the results shown, RAP and CC appear to exhibit lower particle breakdown potential compared with CFM. The increase in fines content for RAP (0.6%) and CC (1.6%) is less than half that for CFM (3.6%). This indicates that RAP and CC are not likely to produce significant amounts of fines during field compaction.

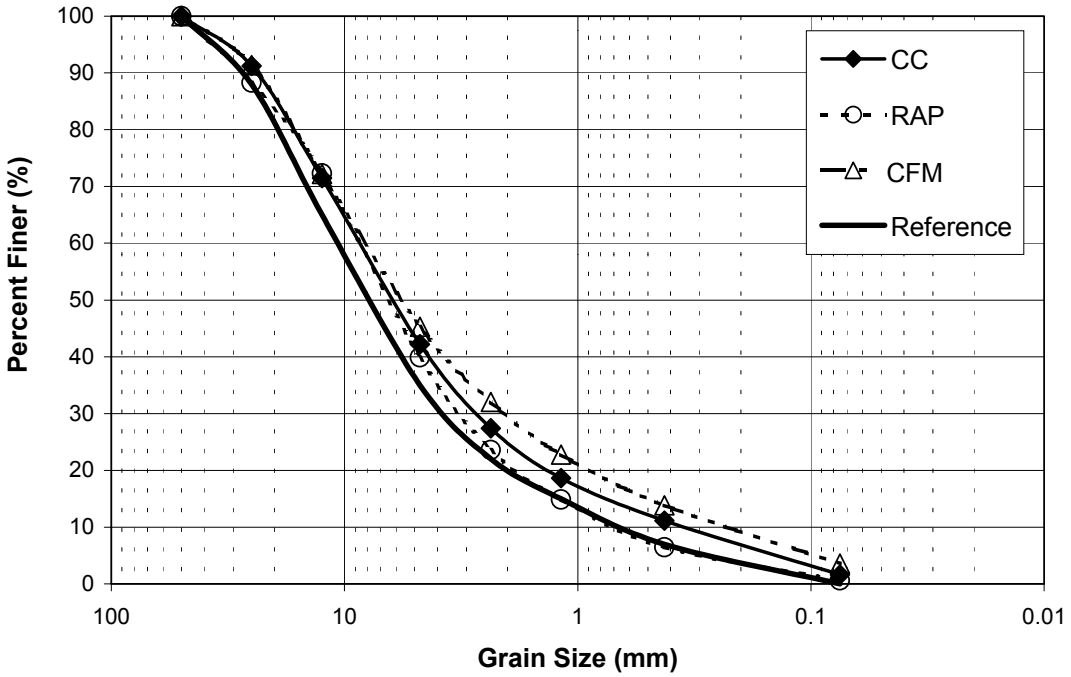

Figure 2.3 Degradation of materials after compaction using the Tex-113-E method.

2.1.5 Relative Density (D_R)

Relative density is determined by measuring the in-place dry density (γ_d) in the field and the minimum and maximum index densities (γ_{min} and γ_{max}) in the laboratory. For the materials evaluated in this study, γ_{min} was measured by placing material into an 11-inch standard mold with a hand scoop to obtain the loosest density (ASTM D4254 - Method A). γ_{max} was measured using the vibratory table method (ASTM D4253). The results are given in Table 2.3 along with the relative density (D_R) of each material corresponding to optimum compaction with the Tex-113-E method (Table 2.2). The relative densities of all three compacted materials are greater than 100% because the energy induced by the Tex-113-E method is much higher than that from the vibratory table.

Table 2.3 Minimum and maximum dry densities of each material and relative density when compacted to optimum conditions with the Tex-113-E method.

Material	γ_{min} *(lb/ft^3)*	γ_{max} *(lb/ft^3)*	*Tex-113-E Compaction*	
			γ_d *(lb/ft^3)*	D_R *(%)*
CC	94.1	110.5	119	141
RAP	90.1	107.8	117	140
CFM	99.8	116.8	125	139

2.2 Field Compaction Control

Control of the backfill compaction during construction of an MSE wall is critical for proper wall performance. The water content during compaction and the compacted density affect the permeability, compressibility, and shear strength of the material, as well as the pullout capacity of the reinforcing elements in the fill. For granular materials, a greater compacted dry density yields a stronger, less compressible material. For backfill materials with significant fines, relatively small variations in compaction water content can adversely affect backfill drainage, compressibility, shear strength, and reinforcement capacity. Further, backfills that are too wet during MSE wall construction can make it difficult to maintain acceptable facing alignment, whereas materials that are compacted too dry may experience excessive settlement upon subsequent wetting (Elias and Christopher 1996).

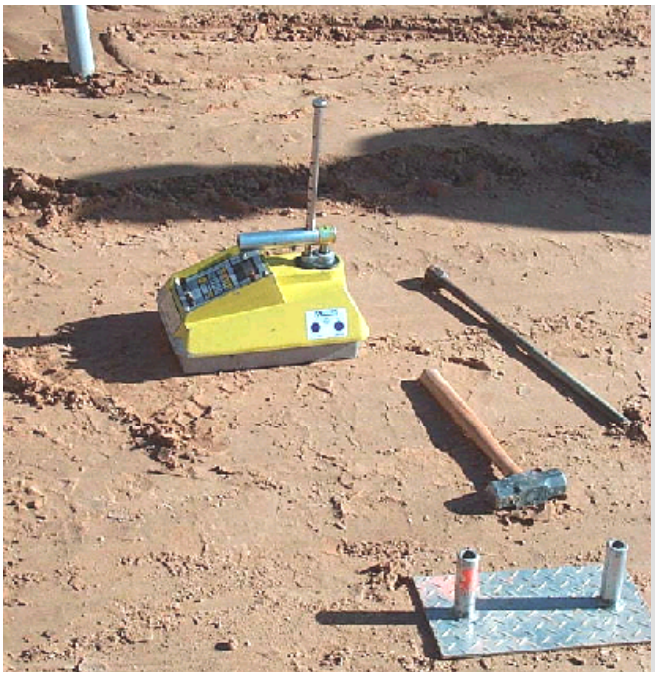

Figure 2.4 Nuclear test gauge for control of compaction in an MSE wall backfill.

Because the compacted dry density and moisture content are critical to the performance of an MSE wall, field density measurements should be performed on a regular basis during backfill construction. For the construction of highway fills, nuclear gauges are widely used to measure in-place density and water content. The use of a nuclear gauge on an MSE construction project is shown in Figure 2.4. Nuclear gauges are popular primarily because the test results can be obtained rapidly. This section describes an experimental investigation conducted to study the accuracy of the nuclear test method in measuring the density and water content of CC, RAP, and CFM (crushed limestone). The following sections describe test methods for measuring field density and water content, the experimental program utilized in this study, and the test results.

2.2.1 Field Density Measurement Methods

Sand cone and rubber balloon (volumeter) methods have long been used to measure the in-place density of compacted material. These conventional methods require the manual excavation of a small test hole and are somewhat time consuming. Water contents are obtained by drying the excavated material in an oven, a step that normally takes 12 to 24 hours and significantly delays the final test results. Nuclear gauges, introduced in the 1950s, provide a more rapid means of measuring in-place density and water content. Much

research has been conducted to study the correlation between densities and water contents measured by nuclear gauges and those measured by conventional methods (e.g., Burati and Elzoghbi 1987; Mamlouk 1988; Kennedy et al. 1989; Sanders et al. 1994; Nagi and Whiting 1999). The following sections describe procedures for the sand cone, rubber balloon, and nuclear gauge tests. The advantages and disadvantages of each method are also discussed.

Sand Cone Method (ASTM D1556) - The sand cone test method is generally accepted as an accurate means of measuring in place soil density (Mamlouk 1988). The test is performed by first excavating a hole in the test material. The excavated material is weighed and stored in a container for later moisture content determination. A dry, uniform reference sand is then poured into the hole. The weight of the sand placed in the hole is measured and, because the density of the reference sand is known, the hole volume can be determined. The moist density is then calculated from the weight of excavated material and the hole volume, while the dry density is computed from the measured moist density and water content. The sand cone method is limited to soils that are stiff enough for an excavated hole to remain open without significant deformation or volume change during the test. In addition, this test works best in unsaturated soils where water will not seep into the excavated hole. One further drawback of this method is the inevitable commingling of the reference sand with the test material after the test is completed.

Rubber Balloon Method (ASTM D2167) - The rubber balloon method is similar to the sand cone method. However, instead of pouring a reference sand into the excavated hole, the hole volume is measured with a water-filled balloon under a calibrated operating pressure. The volume of the water required to fill the hole, and thus the hole volume, is determined from a graduated cylinder. A potentially significant problem with the rubber balloon method is the deformation of the excavated hole during the application of the operating pressure. Expansion of the hole is more pronounced when testing materials that are relatively soft or deformable. Inaccurate results can also be attributed to the presence of rocks or coarse particles that make the hole sides rough, because the balloon may not fill the hole completely if the sides are irregular. Moreover, the test can be difficult to perform in materials containing sharp particles that may puncture the rubber balloon.

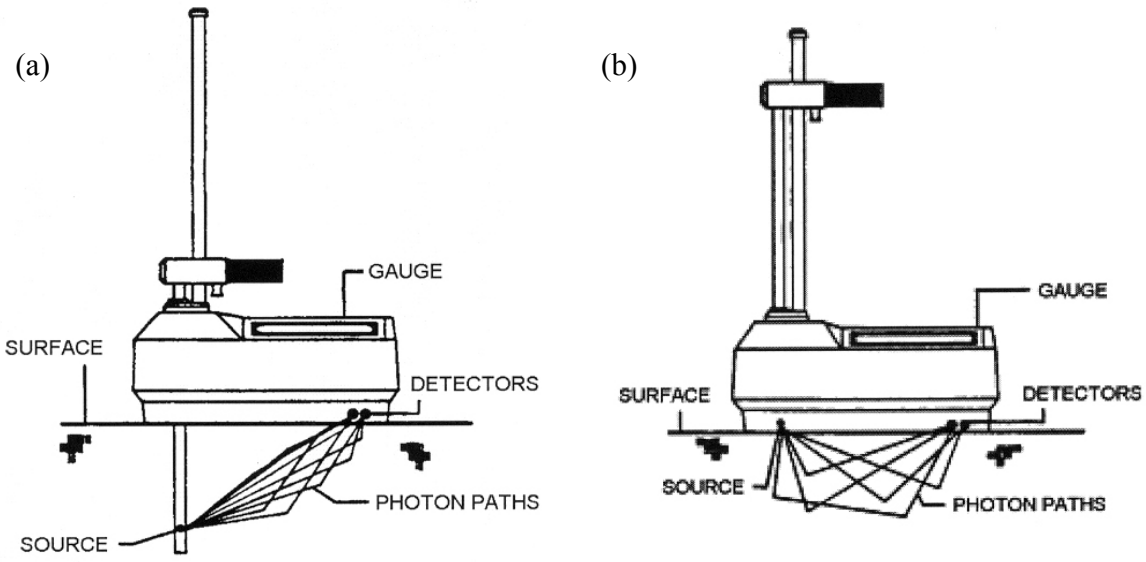

Figure 2.5 Nuclear gauge setup for the (a) direct transmission method and (b) backscatter method (from Troxler 2001).

Nuclear Gauge Method (ASTM D2922 and ASTM D2950) - Over the last 50 years, the nuclear gauge has become a popular tool for measuring soil compaction. Nuclear gauges are also widely used to evaluate asphalt and concrete density. The test method is rapid (less than 5 minutes) and allows repetitive measurements to be made at a single test location. A nuclear gauge obtains concurrent, independent measurements of the moist density and water content of the compacted material. For density measurements, the device employs a small gamma radiation source and one or more gamma photon detectors. The moisture content determination involves a fast neutron source and a thermal neutron detector. There are two modes of operation for the nuclear gauge, routinely referred to as "direct transmission" and "backscatter."

In direct transmission, a rod containing a cesium-137 source is lowered to a predetermined depth (Figure 2.5(a)). Gamma photons emitted by the source travel through the material to the detector, which is located in the base of the nuclear gauge. The density measured by this mode is representative of the material density in the path between the source and the detector (Regimand and Gilbert 1999). For the backscatter mode, the cesium-137 source is placed on the surface of the test material (Figure 2.5(b)). The gamma photons are introduced into the material and must be reflected to reach the detector (Troxler 2001). Because the measured photons are reflected, the average energy of the

photons detected by this method is usually lower than the average energy of the photons detected by the direct transmission method. The density measured in the backscatter method is representative of the average density of the material near the surface.

The nuclear gauge measures density indirectly by counting the emitted gamma photons that reach the detector. While traveling through the soil from the source to the detectors, the gamma photons collide with electrons present in the material. These collisions reduce the number of the photons that reach the detectors. The number of gamma photons reaching the detectors is inversely proportional to the material density (more collisions in higher-density materials mean fewer gamma photons reach the detectors). The number of detected gamma photons is usually referred to as the "count ratio." A calibration relating count ratio to material density is used to determine the material density during testing.

The chemical composition of the material being tested may affect the measured densities, because elements with high atomic numbers will absorb more photons (Nagi and Whiting 1999). Consequently, a calibration developed for one type of material may not yield an accurate result if used to measure density in a different type of material. Accordingly, a calibration should be developed for the particular material to be tested (Kennedy et al. 1989; Nagi and Whiting 1999).

To measure water content, the nuclear gauge emits neutrons, usually from an americium-241 source, into the test material. These neutrons are uncharged and collide with the nuclei of other atoms, which reduces the velocity of the neutrons to a minimum. Neutrons traveling at this minimum velocity are called "thermalized" neutrons. Hydrogen nuclei are most efficient in thermalizing neutrons, so the number of thermalized neutrons is proportional to the mass of hydrogen in the material (Nagi and Whiting 1999; Troxler 2001). Thus, by counting the slow neutrons that reach the detector, one obtains a measure of the number of hydrogen atoms in the material. It is important to note that this number yields a measure of the number hydrogen atoms present, not the number of water molecules (Nagi and Whiting 1999). This can cause errors when measuring the water content of materials that contain significant sources of hydrogen other than water.

2.2.2 Field Testing Program

Tests were undertaken to evaluate the reliability of the nuclear gauge method for routine density and moisture content measurements of CC and RAP during MSE wall construction. More specifically, the study was performed to determine whether the elemental composition of crushed concrete and recycled asphalt pavement affects the accuracy of the nuclear gauge data. Tests in a conventional fill material (CFM), a crushed limestone, were conducted for comparison.

The experimental program was performed on the three material stockpiles located at the Pickle Research Center at the University of Texas at Austin. These stockpiles (Figure 2.6) are the sources for samples to be tested in other phases of this research project. A front-end loader was used to level the top of each stockpile, while maintaining a minimum thickness of about 2 ft within the stockpile. The front-end loader was then driven back and forth on the stockpiles to introduce some degree of compaction in the material. The surfaces of the stockpiles at each test location were then smoothed by hand. The test locations on the CFM, CC, and RAP stockpiles are shown in Figures 2.7, 2.8, and 2.9, respectively. Before testing, some water was introduced to vary the water content at each test location.

Figure 2.6 Testing on the three material stockpiles.

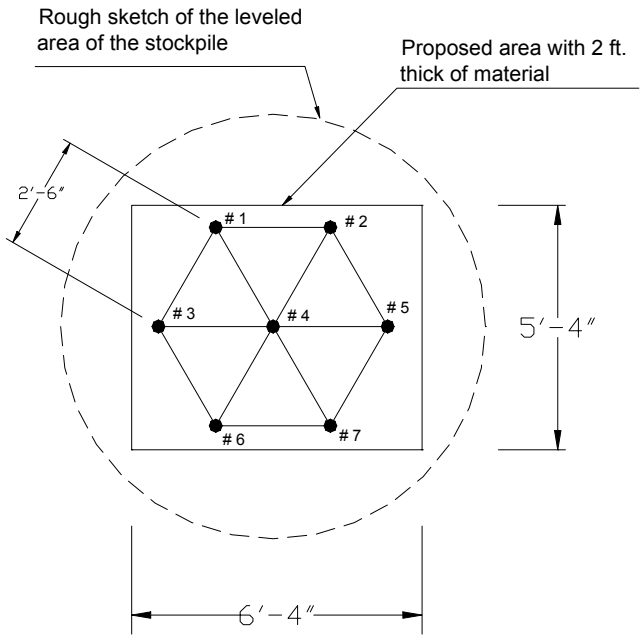

Figure 2.7 Conventional fill material (CFM) stockpile and test locations.

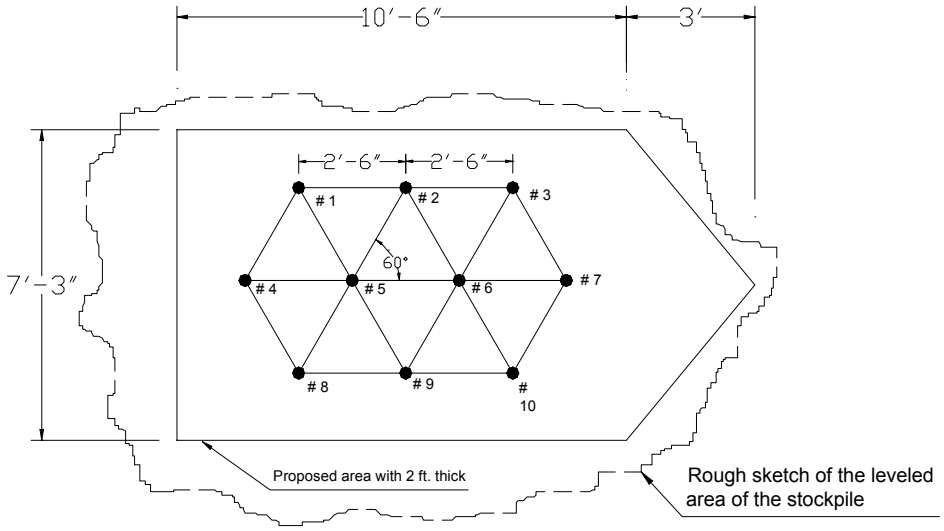

Figure 2.8 Figure 2.8. Crushed Concrete (CC) stockpile and test locations.

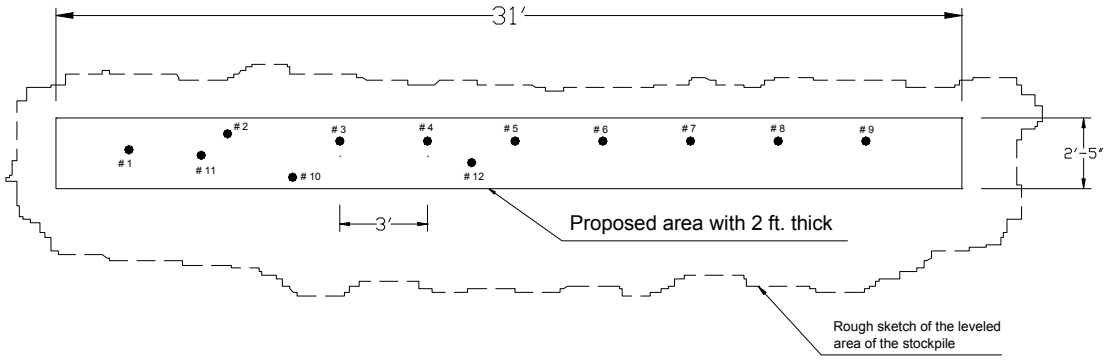

Figure 2.9 Recycled asphalt pavement (RAP) stockpile and test locations.

The experiment was designed to compare moist densities measured with the nuclear gauge with those obtained from the conventional rubber balloon method. For these tests, the rubber balloon method was selected over the sand cone method to avoid mixing sand into the stockpiled material, which will be used in other tests later in the project. Moisture contents obtained with the nuclear gauge were compared with water contents measured by drying the excavated material overnight in an oven at 105°C to 110°C.

Nuclear gauge testing (Figure 2.10) was performed on October 9, 2001, by Trinity Engineering Testing Corporation of Austin, Texas. The nuclear gauge was calibrated in accordance with ASTM D2922. The moist density and water content were measured at each test location with the nuclear gauge using the direct transmission mode. Before performing each test, a scraper plate and rod guide were used to prepare the test location and drive a hole for the instrument rod. The radioactive source on the instrument was then advanced in the hole to a depth of 6 inches.

Figure 2.10 Nuclear gauge tests.

Immediately after the nuclear gauge was removed from the test location, a rubber balloon test was performed. As shown in Figure 2.11, a 4-in. diameter hole was excavated to a depth of about 5 in., with the center of the hole lying directly between the previous locations of the radioactive source and the detector. The excavated materials were weighed and stored in containers for later moisture content determination through oven drying. The volume of the excavated hole was then measured using a rubber balloon apparatus with an applied operating pressure of 4 psi, as seen in Figure 2.12.

2.2.3 Test Results and Discussion

The nuclear gauge and rubber balloon methods were used to measure moist densities and water contents at seven to ten locations within each stockpile. The measurements are compared below.

Figure 2.11 Excavation of hole for rubber balloon test.

Figure 2.12 Rubber balloon test of material density.

Moist Density Test Results - The moist densities of the CFM, CC, and RAP measured by the nuclear gauge and rubber balloon method are compared in Figure 2.13. For each material, the nuclear gauge shows a relatively small variation in the measured densities with all values within ±5% of each other, suggesting that all three stockpiles had a fairly uniform density. The densities measured with the rubber balloon method, on the other hand, show much more scatter. More significantly, the moist density measured by the nuclear gauge was consistently larger than the moist density measured by the rubber balloon method for all three materials.

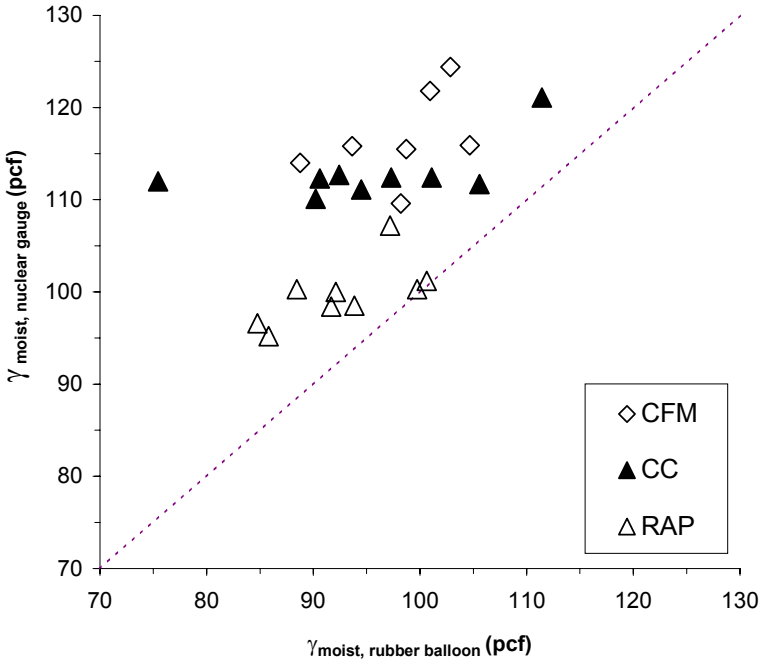

Figure 2.13 Comparison of moist densities measured by rubber balloon and nuclear gauge methods in all three materials.

A comparison of these data can be made in terms of the ratios between the values measured from the nuclear gauge ($\gamma_{m,NG}$) and the values obtained from the rubber balloon method ($\gamma_{m,BAL}$). The average ratio and standard deviation of the ratios of each material tested, as well as the minimum and maximum ratios, are given in Table 2.4. On average, the nuclear gauge reports moist densities 20% higher than the rubber balloon method for

CFM and CC. For RAP, the nuclear gauge is about 10% higher. The scatter in the data is most significant for the CC. These values are larger than those obtained in other studies, which found that the nuclear gauge only slightly overpredicted density (Kennedy et al. 1989; Sanders et al. 1994).

The discrepancies in the test data could be attributed to several factors. It is possible that the soil used to calibrate the nuclear gauge was significantly different from the materials used in this study, making the calibration less accurate. As mentioned previously, calibration of the nuclear gauge with one material may not be appropriate for other materials. For this reason, a calibration curve should be developed for the particular materials on site to ensure accurate results. This is most critical when the test material contains high atomic number elements that affect the gauge count (Nagi and Whiting 1999).

Table 2.4 Ratio of moist densities measured by nuclear gauge ($\gamma_{m,NG}$) and rubber balloon method ($\gamma_{m,BAL}$).

Ratio		*CFM*	*CC*	*RAP*
$\frac{\gamma_{m,NG}}{\gamma_{m,BAL}}$	Average	1.19	1.19	1.08
	Std. Dev.	0.06	0.13	0.05
	Min. to Max.	1.11 to 1.28	1.06 to 1.48	1.01 to 1.14

Two other factors may contribute to unsatisfactory comparisons of measured densities. First, the excavated hole may have expanded under the applied operating pressure during the rubber balloon test. Deformation of the hole would lead to a larger measured hole volume and a lower soil density. The measured densities from the rubber balloon method are all lower than those from the nuclear gauge, indicating that this error is consistent with the observations. However, the field material was stiff and most likely did not deform significantly under the balloon pressure.

The presence of large-size particles is a second factor that may have contributed to the observed errors. When the test material contains large particles or large voids, irregularities may occur in the source-detector path of the nuclear gauge and cause higher or lower measured densities. To minimize this problem, multiple nuclear gauge tests should be run at adjacent locations to get an average result (ASTM D2922). However, even

though the stockpiles were not compacted uniformly, the nuclear gauge data in Figure 2.13 exhibit relatively little scatter, especially in the RAP and CC results. Large particles also affect the rubber balloon test results if the excavated hole is too small to adequately sample all particle sizes. Therefore, ASTM D2167 specifies larger hole volumes for materials with larger particle sizes. Unfortunately, the holes used in the rubber balloon tests in this study were not large enough for the particle size distribution of the test materials. This may have adversely affected the densities measured with the rubber balloon method.

The possible effect of the large particles on the rubber balloon densities was studied further by measuring density using the water displacement method (ASTM D5030) in small, plastic-lined test pits in the RAP. This test method is based on the same principle as the rubber balloon test, but the material sample is significantly larger and no operating pressure is applied to the test pit. Three test pits, each about 1 ft^3 in volume, were excavated in the RAP stockpile to measure moist density. For comparison, rubber balloon tests were performed adjacent to the test pits. The moist densities measured by the test pit and rubber balloon methods are compared in Figure 2.14. The data do not indicate a consistent relationship between the densities obtained with the two test methods. However, the rubber balloon method produced smaller densities in two of three locations, possibly because the small hole for the rubber balloon test did not adequately sample all particle sizes.

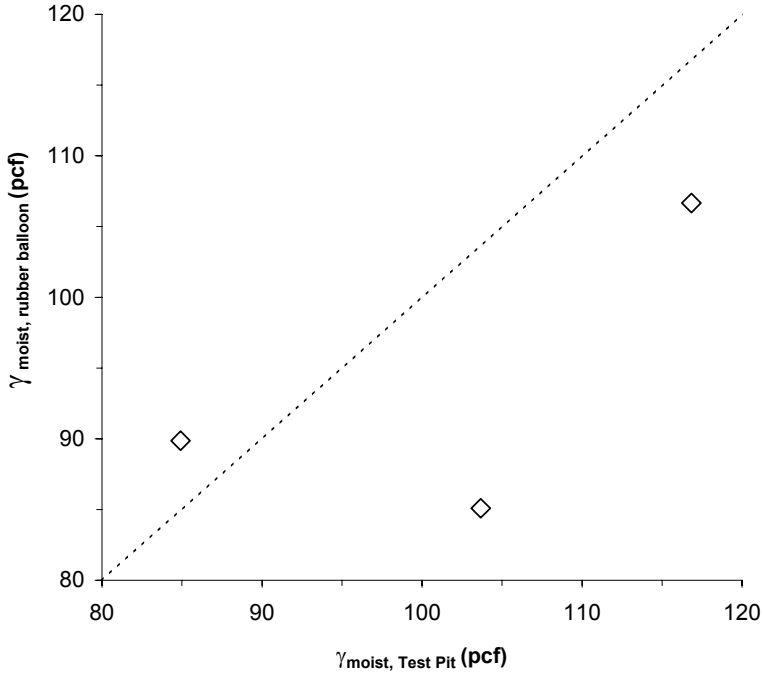

Figure 2.14 Comparison of moist density of RAP measured by rubber balloon and test pit methods.

Moisture Content Test Results - The moisture contents of the CFM, CC, and RAP stockpiles measured with the nuclear gauge and by oven drying are compared in Figure 2.15. Table 2.5 shows the ratio of water contents measured by the two methods for each material. Compared with the oven-dried values, the nuclear gauge gives acceptable results for the CFM with an average ratio of 0.99. Moisture contents measured by the nuclear gauge for CC are slightly higher (about 20% higher, on average) than the values measured by oven drying. For RAP, the nuclear gauge moisture contents are much higher. On average, the nuclear gauge reports water contents in the RAP that are three times greater than that obtained by oven drying.

Table 2.5 Ratio of moisture contents measured by nuclear gauge (w_{NG}) and oven drying (w_{OVEN}).

Ratio		*CFM*	*CC*	*RAP**
$\frac{w_{NG}}{w_{OVEN}}$	Average	0.99	1.19	3.07
	Std. Dev.	0.12	0.10	0.69
	Min. to Max.	0.84 to 1.19	1.03 to 1.33	2.36 to 4.51

* One anomalous data point with a ratio of 15.7 was removed from the RAP data set.

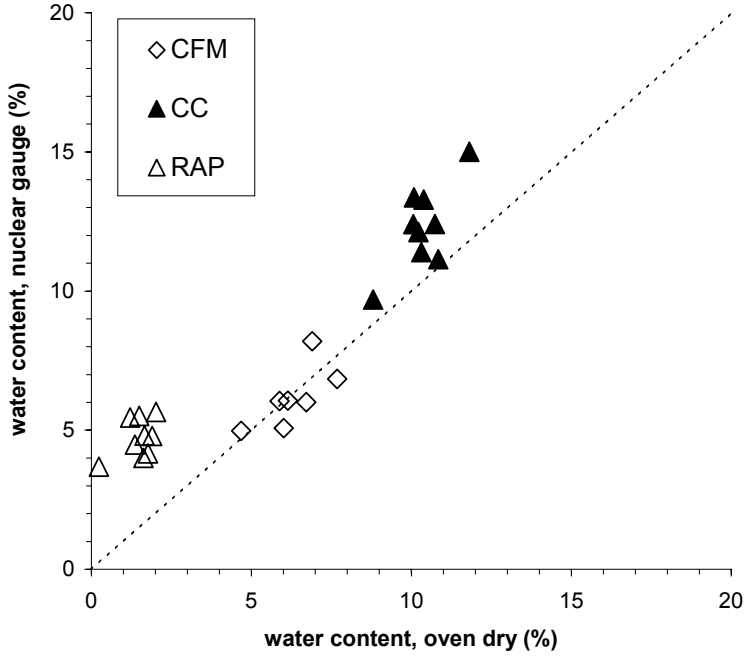

Figure 2.15 Comparison of the moisture contents measured with the nuclear gauge and oven drying.

The nuclear gauge apparently overestimates the moisture content in the CC and RAP because it measures the amount of hydrogen in the material and not the amount of water. The slightly higher measured water contents in CC may result from the additional hydrogen atoms in the admixtures, modifiers, and cement paste (Nagi and Whiting 1999). In RAP, the residual bituminous cement, a petroleum product comprised of a mixture of

hydrocarbon molecules, is clearly a major source of hydrogen (Black 1995). The hydrogen in the asphalt binder appears to cause the nuclear gauge to report very high water contents in RAP.

Because the elemental composition of the material affects the moisture contents reported by the nuclear gauge, separate calibrations for RAP and CC are needed to obtain accurate measurements of compaction water content. Because the measurements in RAP appear to be sensitive to the hydrogen content of the asphalt, it may not be feasible to develop a generic calibration for measuring compaction water content in RAP with the nuclear method. Rather, field calibrations at each project site may be necessary to obtain reliable water contents in RAP from the nuclear gauge.

2.2.4 Conclusions from Field Compaction Control Tests

The suitability of the nuclear gauge for measuring the moist density and water content of CC, RAP, and a crushed limestone (CFM) was evaluated in a series of field tests on three stockpiles of material. The nuclear gauge consistently measured larger densities than the rubber balloon method, although these measurements may have been affected by large particles in the test materials. Given the uncertainty associated with the rubber balloon measurements, it is difficult to judge conclusively the accuracy of the nuclear gauge data in these evaluation tests.

Elemental composition of the material can have a major influence on the moisture content measured by the nuclear gauge. Because the nuclear gauge measures hydrogen atoms rather than free water molecules, the values of water content measured by the nuclear gauge were higher than the oven-dried values for CC and RAP. This effect was particularly pronounced in the RAP, where large amounts of hydrogen are contained within the residual asphalt binder.

Overall, the test results indicate that the nuclear gauge measurements are material dependent. Because many factors affect nuclear gauge measurements, frequent field verification of nuclear gauge results are recommended. Separate calibrations should for developed for RAP and CC, especially for determinations of water content from the nuclear gauge method.

2.3 Preliminary Results from Triaxial Tests

An initial series of thirteen consolidated-drained triaxial compression tests has been completed on compacted specimens of CC, RAP, and CFM. Four tests were performed on CC and CFM specimens and five were conducted on RAP. The effective confining pressures ranged from 12 to 45 psi (83 to 310 kPa). Additional tests are currently underway to further validate the measured shear strengths of these materials.

2.3.1 Specimen Preparation and Testing Program

A consistent reference gradation (Figure 2.1) was selected for the preparation of all test specimens. However, standard practice in geotechnical testing requires that the largest particle size in a triaxial test specimen must not exceed one-sixth of the specimen diameter. Given the 4-in. (100 mm) specimen diameter for the UT triaxial apparatus, all particles larger than 0.67 in. (17 mm) were removed. This scalping was accomplished by using only material that passed a 0.63 in. (16 mm) sieve, which resulted in the specimen gradation indicated in Figure 2.15 (solid line). All of the RAP, CC, and CFM triaxial specimens were manually mixed to the gradation shown in Figure 2.16.

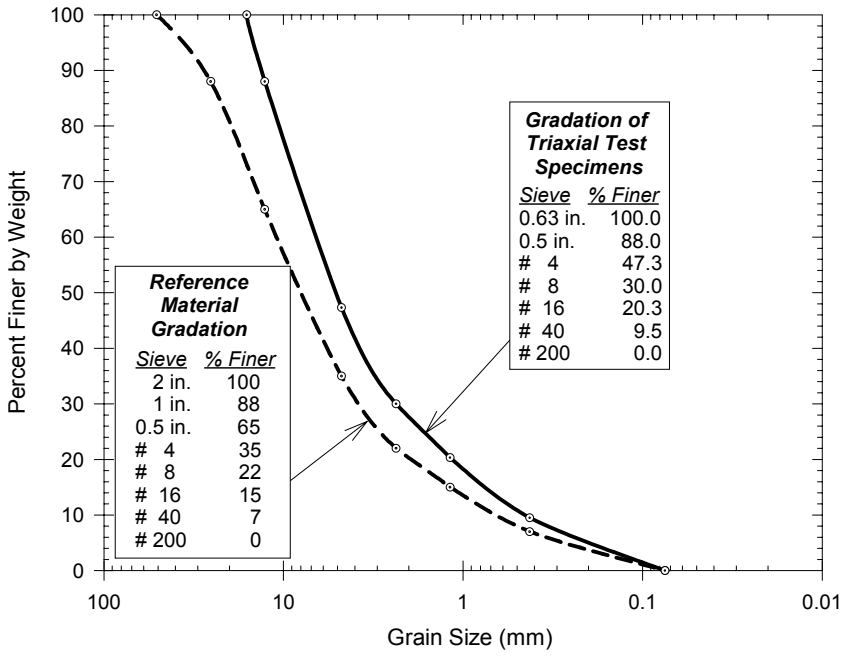

Figure 2.16 Grain size distribution of reference material and triaxial test specimens.

All tests were conducted with a computer-controlled load frame on 4-in. diameter specimens in a triaxial cell. The specimens were compacted in a mold 4 in. in diameter by 8 in. high (100 mm by 200 mm), using a compaction energy per unit volume that was equivalent to the Tex-113-E method. After removing the compacted material from the mold, a rubber membrane with a thickness of 0.025 in. (0.64 mm) was placed around the specimen and secured to the end platens using O-rings. The test cell was then assembled and an initial confining pressure of approximately 5 psi (35 kPa) was applied to the specimen. Water was then slowly flushed from the bottom up through the specimen to fill the voids and displace as much pore air as possible. This process was continued until no air bubbles were visually detected in the drain lines connected to the top of the specimen.

The specimens were then pressure saturated by raising the cell pressure and the applied pore water pressure (backpressure) in increments. The capacity of the test equipment limited the maximum cell pressure to 106 psi (731 kPa). The final B values (B = change in pore pressure per change in confining pressure, Skempton 1954) ranged from 0.80 to 0.92. Larger B values indicate specimens with a higher degree of saturation. Various procedures were attempted to increase the saturation (as indicated by the final value of B), including leaving the specimens under high backpressures for 24 hours and flooding the specimens under vacuum; however, these practices did not lead to significantly higher B values.

After saturation, hydraulic conductivity tests were performed on the specimens. A difference in water head between the top and bottom of the specimen was imposed to create a hydraulic gradient and the resulting flow rate through the specimen was measured. The final step was a consolidated-drained triaxial compression test performed on the same specimen. Various effective confining pressures were applied to the specimens prior to shearing. The strain rate was set at 1% per minute for all tests, a rate sufficiently slow to allow full drainage of excess pore pressures during shearing. All test data were recorded electronically.

2.3.2 Hydraulic Conductivity

Before shearing the test specimens in triaxial compression, the hydraulic conductivity was measured. Both the CFM and RAP exhibited relatively high permeabilities, but the initial tests indicated a much lower hydraulic conductivity in the crushed concrete. It is

possible that CC is not as freely draining as the other two materials because hydration of the residual cement paste blocks pores in the compacted material. However, given the inherent variability in the hydraulic conductivity of compacted materials of this kind, more data are needed to substantiate the observed results. Additional tests, including both flexible wall tests in a triaxial cell and fixed wall permeameter tests, are being conducted to further characterize the hydraulic conductivity of CC and RAP.

2.3.3 Drained Shear Strength

Results from the consolidated-drained triaxial compression tests on all three materials are plotted in terms of deviator stress ($\sigma_1 - \sigma_3$) and volumetric strain (ε_v) versus axial strain (ε_a) in Figure 2.17. The deviator stress was computed by dividing the applied axial load by the current cross-sectional area of the specimen, assuming a right circular cylinder area correction. Failure was defined as the peak stress difference ($\sigma_1 - \sigma_3$) in each test. The shear strength properties measured for all three materials are summarized in Table 2.6.

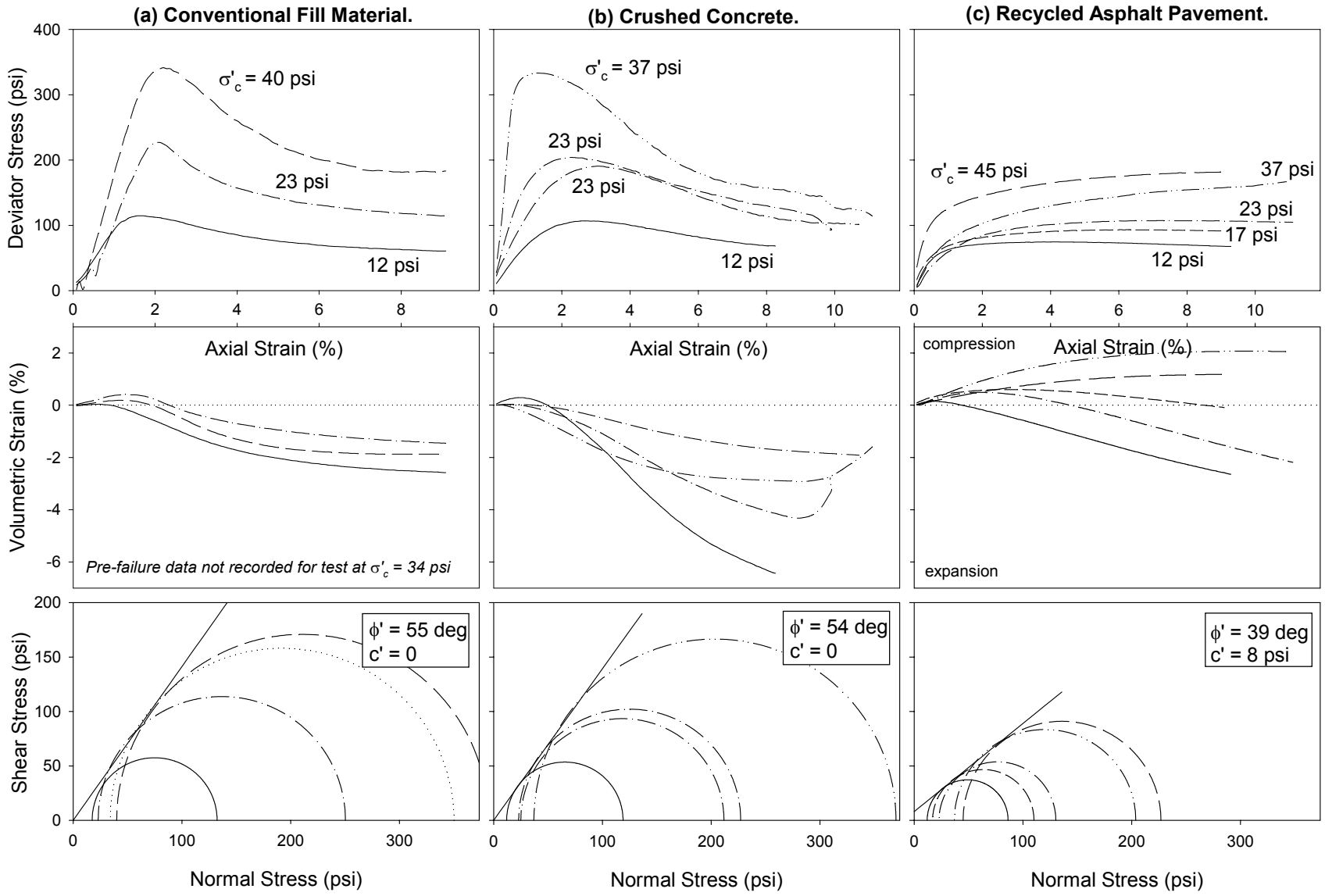

Figure 2.17 Results from consolidated drained triaxial tests on the test materials.

Table 2.6 Summary of preliminary drained strength properties.

	CFM	*CC*	*RAP*
Effective Confining Pressure Range (psi)	12 – 40	12 – 37	12 – 45
Effective Stress Friction Angle, ϕ'	55°	54°	39°
Effective Cohesion, c' (psi)	0	0	8

Conventional Fill Material – Tests on CFM were performed at effective confining pressures ranging from 12 to 40 psi (83 to 276 kPa). All of the CFM specimens exhibited strain-softening behavior (Figure 2.17(a)), reaching a maximum deviator stress at approximately 2% strain and then declining to a residual value. Each specimen experienced between 1 and 2% expansion at the end of testing. Additionally, all of the CFM specimens displayed a distinct failure plane through the specimen during shear. This response is typical for a dilative material in drained shear. The effective friction angle based on these four tests is 55°, with a cohesion intercept of zero.

Crushed Concrete - Tests on CC were performed at effective confining pressures ranging from 12 to 37 psi (83 to 255 kPa). All specimens exhibited strain-softening behavior (Figure 2.17(b)), reaching a maximum deviator stress at approximately 2% strain and then declining to a residual value. The CC specimens experienced between 2 and 6% expansion at the end of testing, with the most dilation occurring at the smallest confining pressure. As with the CFM, all specimens displayed a distinct failure plane through the specimen during shear. The effective friction angle based on these four tests is 54°, with a cohesion intercept of zero.

Compared with the conventional fill material, the crushed concrete has similar shear strength properties. Both the CFM and CC are highly angular materials with relatively high drained friction angles at confining pressures up to 40 psi (275 kPa), although lower friction angles can be expected at higher confining pressures. Also, because the tests reported here were conducted on specimens in which all particles larger than 0.63 in. had been removed, the strength of the composite material may be somewhat lower, as the

largest particles of this crushed material may be more fractured. While additional tests are warranted, the shear strength of CC appears to be adequate for MSE wall backfills.

In addition, during the preparation of one CC test specimen, some visual evidence was noted that suggests unhydrated cement paste may be present in the crushed concrete. Subsequently, several samples of uncompacted, wet CC were dried overnight in an oven. Upon removal from the oven, the material had a distinct, hardened crust. The individual aggregate grains were noticeably conglomerated, forming larger chunks of cemented material that were visibly different from the original material. It is possible that bonding occurred due to hydration of cement paste in the crushed concrete. If true, then the strength of compacted CC may increase somewhat with time following compaction. Only freshly compacted material was evaluated in the preliminary test series, so this effect is minimal in the test data presented here. More testing is needed to study this potential phenomenon.

Recycled Asphalt Pavement - Tests on RAP were performed at effective confining pressures ranging from 12 to 45 psi (83 to 310 kPa). All tests exhibited strain-hardening behavior (Figure 2.17(c)), with the deviator stress continuing to rise or remaining steady throughout the duration of the test. Volumetric strains ranged from expansive to contractive, depending on the confining pressure, in contrast to the dilative volumetric strains observed in the tests on CFM and CC. Additionally, no specimens displayed a distinct failure plane during shear. Rather, the specimens compressed vertically and exhibited a slight radial bulge near the center as the axial load was applied. This behavior is typical for a contractive material in drained shear. It is somewhat surprising that compacted specimens would exhibit contractive behavior at these confining pressures. The contractive behavior may be the result of the bitumen preventing dense packing of the RAP particles during compaction, and indicates that RAP fills may be susceptible to compression settlements if the material is not adequately compacted during construction.

The effective stress friction angle based on these five tests is 39°, with a cohesion intercept of 8.0 psi (55 kPa). Although the measured shear strength of RAP was lower than that for the conventional fill material, the RAP tested appears to exhibit adequate strength properties to be used as a backfill material. The observed cohesion ($c' = 8$ psi) likely results from the residual bitumen bonding the particles together. However, it is not clear if this

component of shear strength can be relied upon for design. The lower friction angle for RAP, compared with that of CFM, may result from more rounded aggregate particles or from reduced interparticle friction due to the residual bitumen in the RAP. Additional studies are needed to assess the stability of this material, particularly to determine whether RAP is susceptible to creep failure at large shear stress levels. As with the crushed concrete, additional studies are needed to evaluate whether the removal of particles larger than 0.63 inch from these test specimens had a significant effect on the measured strength.

2.4 Design and Construction of the Large Direct Shear Machine

As pointed out in Section 2.3.1, the larger particles must be removed from the CC and RAP before these materials can be tested in the triaxial device. Scalping of the larger particles may lead to an unrepresentative, higher shear strength in the triaxial tests, as the largest particles in a crushed material tend to be weaker and more prone to deterioration when sheared. To evaluate the shear strength of the full reference gradation of these materials, which includes particles up to 2 in. in size, the large direct shear machine depicted in Figure 2.18 was designed and built. The design of this test apparatus is described in this section.

Standards for direct shear testing (ASTM D3080) require that the test specimen have a width at least ten times the largest particle size and a thickness equal to one-half of the width. Hence, to test the full reference gradation of CC and RAP, the direct shear machine was designed to test compacted samples of CC and RAP measuring 20 in. by 20 in. in plan and 10 in. thick. Tests will be performed at different confining pressures on specimens compacted using an energy equivalent to the Tex-113-E test method with an optimal water content as given in Table 2.2.

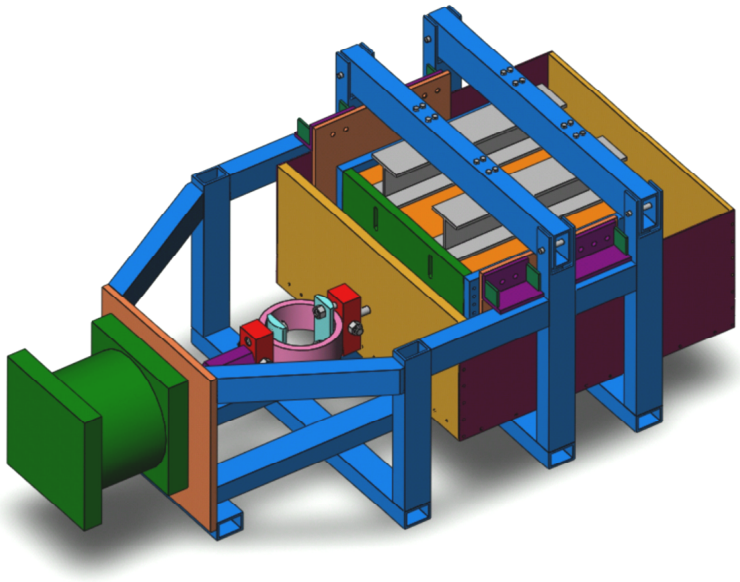

Figure 2.18 Three-dimensional, schematic drawing of the large direct shear test machine (courtesy of Hi-Tech Products, Inc.)

The large direct shear machine includes a water tank (Figure 2.19) for submerging the compacted test sample, which eliminates capillary stresses that affect the measured shear strength. During the test, the upper half of the shear box is held stationary while the lower half is pulled horizontally. As seen in Figure 2.19, the lower half of the shear box and the surrounding water-filled tank ride on tracked, low-friction bearings. Normal stresses of up to 50 psi are applied to the test specimen using a square rubber bladder pressurized with air. This normal stress is commensurate with the stress levels in the backfill of a 55 - 60 ft high MSE wall. Horizontal shear forces are generated using a single 12-in. diameter pneumatic piston with a 5-in. stroke. Operated with pressures up to 250 psi, delivered from a tank of bottled air, the piston can deliver over 20,000 lb of shear force. The machine will be used to conduct stress-controlled tests, where constant normal and shear forces can be maintained for long periods of time, as needed to assess creep behavior. Operation of the direct shear machine with pneumatic pressure regulators allows for simple, accurate control for tests of this type. All data from the tests will be recorded manually using a pressure gauge for the normal stress, a proving ring for the applied shear force, and dial gauges for the horizontal and vertical displacements.

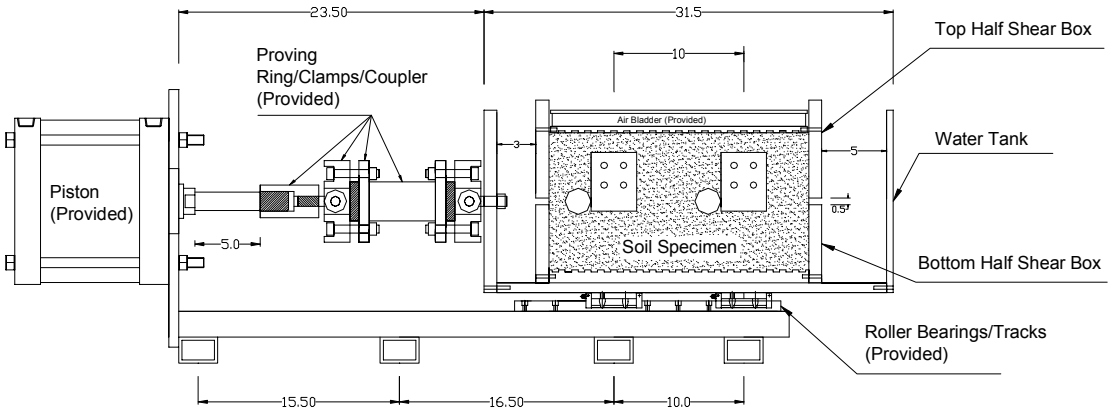

Figure 2.19 Vertical cross-section of the large-scale direct shear test machine.

In addition to the measurement of drained shear strength, data from these tests will be used to assess the potential for post-construction settlement in these backfill materials. Vertical compression of the specimen will be measured during application of the normal stress and during subsequent submergence in water. The large scale of these test specimens provides a unique opportunity to assess this behavior in the laboratory using a representative sample gradation.

With minor modifications, this test machine will also be used to test the pullout resistance of MSE wall reinforcing elements in CC and RAP. These tests will require the design of a clamp to grasp the reinforcement and the addition of dial gauges to monitor deformation along the length of the reinforcement. A number of published studies suggest that test boxes measuring at least 3 ft (1 m) long are required to accurately characterize the pullout resistance of soil reinforcements. However, meaningful data can be obtained from the 20 in. by 20 in. test machine by comparing the pullout resistance of elements placed in CC or RAP and those placed in CFM.

The completed test machine will be unique, given its large size, ability to conduct tests with sustained normal and shear forces (needed for evaluating creep under constant stress conditions), and capability for conducting reinforcement pullout tests. The test machine is currently nearing completion at Astro Mechanics, a machine shop located in

Round Rock, Texas. The final delivered cost of the test machine is estimated to be about half the cost of commercial direct shear machines of similar size.

3. Durability of Crushed Concrete

Deleterious materials and harmful impurities in CC may affect the durability of CC backfill. Recycled CC from structures that have suffered from alkali-silica reaction (ASR) and sulfate attack may still be susceptible to expansion after compaction. Because only limited work has focused on assessing the durability of CC when used as a backfill for MSE walls, research was needed to evaluate the potential issues related to using CC that previously showed poor durability in its originally intended use. To investigate the effects of these attacks on the performance of compacted backfill, concrete was produced in the laboratory and used for accelerated expansion tests. Results from laboratory-produced concrete were then compared with tests performed on CC from commercial producers.

3.1 Background

Three essential components are necessary for ASR-induced damage in concrete: (1) reactive silica (from aggregates), (2) sufficient alkalies (mainly from Portland cement) and (3) sufficient moisture. The reaction occurs between the hydroxyl (OH^-) ions in the pore solution and certain siliceous components of the aggregates. The presence of high concentrations of sodium and potassium alkalies in the pore solution results in an equally high concentration of OH^- ions. It is this high OH^- concentration, and thus high pH, that leads to the initial breakdown of reactive silica components in the aggregates. The alkalies ultimately contribute to the formation of expansive ASR gel, which absorbs water and leads to cracking.

In the case of sulfate attack, Portland cement concrete is attacked by solutions containing sulfate, such as some natural water or polluted ground waters. Attack can lead to strength loss, expansion, spalling of surface layers, and ultimately disintegration. Na_2SO4 and $MgSO_4$ in the attacking solution will react with the cement paste resulting in the formation of ettringite and gypsum. Of concern to MSE facing walls is the expansion that may result due to absorption of water by the ettringite.

Both ASR and sulfate attack have been observed in concrete structures in Texas, so it is anticipated that damaged structures may ultimately be removed and recycled. These deterioration mechanisms involve deleterious expansion, and such expansion could prove

to be damaging in MSE applications. Water is a key instigator of these problems, and backfill with good drainage conditions may be sufficient to mitigate potential problems.

In actual MSE wall construction, recycled fill materials will be exposed to percolating rainwater. Chemical concentrations in the rainwater may contribute to the reactions in the recycled material. For this reason, seasonal precipitation-weighted mean concentrations were collected for several locations in Texas. An average sulfate concentration of 1.215 mg/L was estimated for Texas rainwater. Based on standards developed by the U.S. Bureau of Reclamation, concentrations of soluble sulfates greater than 150 mg/L SO_4 in water endanger concrete (ACI Building Code 318-02). Tests were also done to establish the total alkali (0.05%, 500mg/l) and total sulfate (0.38%, 3800 mg/l) content of the commercial CC. This information will be used, along with ASR and sulfate test exposure solution concentrations, for discussions in the conclusion section.

For the durability tests, a single reference gradation was used for all CC sample preparation. This is the same reference gradation discussed in Chapter 2 and shown in Figure 2.1. To prepare the reference curve, gradation analysis was done on recycled materials from the producer companies and TxDOT districts. Because of the varying gradation of these materials, a single reference gradation was chosen for use in all future testing. The reason for using a single gradation was to eliminate the effect of varying the grain size distribution on test results. The reference gradation limits the maximum particle size to 5 cm (2 in) and allows no fines passing the 0.075mm (0.0029 in) sieve. Note that a slight variation exists for the hydraulic conductivity samples because of scalping of materials greater than 1.9 cm (3/4 inch) from the reference gradation (ASTM D2434).

Compacted backfill materials must be free draining to ensure that excessive pore water pressures are not developed behind the retaining structure. Backfill drainage and soil resistivity are commonly used as indicators for corrosivity. A poorly draining material may be defined as a material with a hydraulic conductivity less than 100 x 10^{-6}cm/sec (Carter and Bentley 1991). Moreover, poorly drained soils having a resistivity less than 1000 Ωm may be highly corrosive (Jones 1996). On the other hand, well-drained soils will tend not to collect moisture, thus ensuring low reinforcement corrosion rates. In addition, since moisture is needed for expansion in ASR and sulfate attack, a well-drained soil may result

in reduced expansion levels. Gradation specifications have been developed for conventional fill materials to ensure that free drainage is achieved (Table 3.1). It is important to study the hydraulic conductivity of recycled materials under these requirements.

Table 3.1 TxDOT and FHWA MSE Wall Backfill Specifications

Requirement	TxDOT (Type A)	TxDOT (Type B)	FHWA
Gradation			
Maximum size	75 mm	150 mm	100 mm
% passing 75 mm sieve	-	75-100	-
% passing 0.43 mm sieve	0-60	-	0-60
% passing 0.075 mm sieve	0-15	0-15	0-15
Plasticity Index (PI)	-	-	<6
Compaction			
Dry Density	95% (Tex-114-E)	95% (Tex-114-E)	95% (AASHTO T-99)
Moisture Content	±2% of w_{opt}	±2% of w_{opt}	within 2% dry of w_{opt}
pH	5.5-10	5.5-10	5-10
Resistivity (ohm-cm)	>3000	>3000	>3000

Remarks: Type B fill that does not meet the 0.075 mm sieve requirement may be used if:

- Less than 25% passes sieve 0.075 mm
- PI ≤ 6
- At 95% dry density (Tex-114-E) and w_{opt}, $\phi \geq 34°$ (Tex-117-E)

Compaction tests were conducted using the Tex-113-E method and the results are reported in CTR Research Report 4177-1 (Rathje et al. 2001). The Tex-113-E method imparts a compaction energy of 111,776 m-kg/m^3 (22,900 ft-lb/ft^3), where:

$$\text{Compaction Energy} = \frac{(hammer\ \ weight)(drop\ \ height)(\#layers)(\#blows/layer)}{(total\ \ volume\ \ of\ \ specimen)} \qquad (3.1)$$

The samples prepared for durability testing were compacted in two layers in steel molds measuring 15.2 cm in diameter by 11.7 cm high (specimen volume = 2095 cm^3). Using a 4.54-kg hammer dropped 46 cm each blow, 57 blows were applied to each layer to achieve the desired compaction energy. The specimens were mixed at a water content of

10%, which was found to yield a maximum dry unit weight with the Tex-113-E method (Rathje et al. 2001).

3.2 ASR Testing Using Crushed Concrete

The ASTM C1293 test method is intended to assess the potential for deleterious expansion of concrete due to either fine or coarse aggregate in an alkaline environment. In this test method, concrete prisms are stored over water at 38°C and expansion is measured at regular intervals. Expansion exceeding 0.04% in one year indicates potentially reactive aggregate.

Previous tests done on ASR at the University of Texas at Austin indicated that a particular fine aggregate from El Paso is very reactive. As a result, the sand was selected as the aggregate to be used in the concrete. Also, a local nonreactive coarse aggregate was selected for use in the mixture. The objective was to test expansion of the compacted CC, recycled from a possible worst-case concrete mixture.

Concrete was prepared for ASR testing in accordance with ASTM C1293, which specifies that a cement content of 420 $\pm$ 10 kg/m^3 be used in the mixture proportions. Also, the volume of coarse aggregate per unit volume of concrete is required to be 0.70 $\pm$ 0.2%, and the water-cement ratio should be maintained in the range of 0.42 to 0.45 by mass. Also, ASTM C1293 specifies an alkali content of 1.25% Na_2O equivalent, by mass of cement, for testing of expansion due to ASR. Since the binder used for the concrete mixture was Type-I Portland Cement, with an alkali content of 0.95%, it was necessary to calculate the additional amount of NaOH needed to increase the alkali content of the concrete from 0.95% to 1.25%. Concrete mixture proportions are shown in Table 3.2.

Table 3.2 ASR Concrete Mixture Proportions (per m3 of concrete, w/c=0.45, ACI 211)

Materials	Kg	BSG* (SSD)	AC**(OD)	Remarks
Cement	322	3.15	NA	ASTM Type-1 Cement
Water	145	1	NA	
NaOH	1.23	-	-	ASTM C 1293
Coarse Aggregate	896	2.62	0.8	ASTM C 33
Fine Aggregate	423	2.59	0.8	ASTM C 33

Determination of Alkali Content, ASTM C 1293

Cement used – Type 1 Portland cement, 0.95% alkali content

Amount of cement in concrete $322 kg/m^3$

Amount of alkali in concrete ($382 kg/m^3$ x 0.95%) 3.06 kg

Specified alkali in concrete ($382 kg/m^3$ x 1.25%) 4.02 kg

Alkali to be added to concrete 0.96 kg

Factor to convert Na_2O to H_2O:

$Na_2O + H_2O \Rightarrow 2NaOH$

Compound	Molecular Weight
Na_2O	61.98
NaOH	40.00

Conversion factor: 2 x 40.00 / 61.98 = 1.29

Amount of NaOH required: 0.96 x 1.29 = $1.23 kg/m^3$

*BSG = Bulk Specific Gravity

**AC = Absorption Capacity

After mixing, all of the fresh concrete was cast into thirty-three 7.6 by 7.6 by 25.4 cm steel molds and three 10.2 by 20.4 cm cylinders, and consolidated to ensure uniform consistency. After curing for a day, the samples were unmolded and moist cured at 23ºC. The prisms were then used for ASR expansion tests, while the cylinders were tested for compressive strength at different time intervals. Compressive test results for the three 10.2 by 20.4 cm concrete cylinders produced an average of 35,853 kPa (5200 psi) at 28 days.

ASR concrete prisms were then divided into two groups. One set of prisms (1 to 18) was moist cured for one day before being subjected to the ASTM C 1293 accelerated ASR prism expansion test at an elevated temperature of 140ºC. The objective here was to expose this group of prisms to expansion levels above the 0.04% expansion limit set in the ASTM standard. These were then used to produce CC that had undergone extensive ASR attack.

To compare the expansion of compacted crushed concrete previously exposed to large chemical attack with that of concrete that had not been exposed to attack, a second set of prisms (19 to 33) was moist cured at 23ºC until the accelerated expansion test on the first set of ASR prisms was completed.

3.2.1 Concrete Prism Test (Modified ASTM C 1293)

Expansion due to ASR in concrete prisms was measured in accordance with the ASTM C 1293 standards. Prisms 1 to 18 were stored in 19-liter buckets with airtight leads to prevent loss of moisture due to evaporation. A perforated rack was placed in the container so that the prisms were 3 to 4 cm above the bottom. The container was then filled with water to a depth of 2 ± 0.5 cm. Also, an absorbent material was placed around the inside wall of the container from the top with the bottom of the wick extending into the reagent water, which allowed for the moisture to uniformly surround the expansion prisms. The buckets were then stored in a 60°C chamber and allowed to expand.

A length comparator was used to measure expansion of the ASR prisms. Initial length readings were made before placing the samples in the chamber. Thereafter, subsequent length readings were taken at weekly intervals and graphs plotted of expansion versus age. As discussed earlier, an aggregate is classified as potentially deleterious to concrete if the average expansion of test specimens is equal to or greater than 0.04% after one year (ASTM C1293). For this reason, prisms 1 to 18 were allowed to expand to levels above the 0.04%, i.e. 0.23% after 42 days (Figure 3.1) before they were crushed for testing as CC. After the expansion observation was stopped for prisms 1 to 18, the lengths of prisms 19 to 33 were measured and the percent expansion was calculated. Figure 3.2 shows an average expansion of 0.015% for these prisms, which is much lower than the ASTM limit of 0.04%.

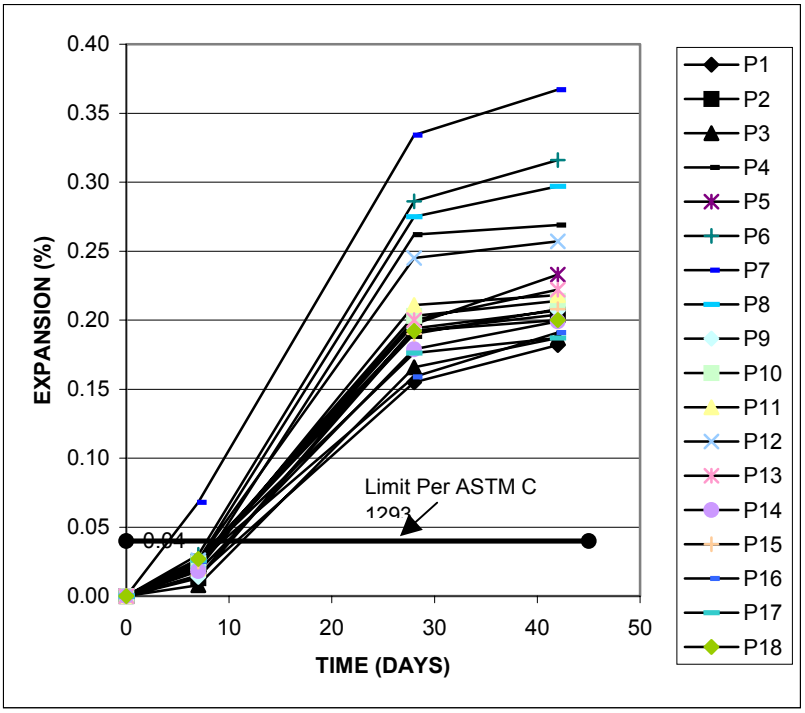

Figure 3.1 Expansion of Prisms 1 to 18, Exposed to Alkali Solution for 42 days, Stored in 60 °C Control Chamber

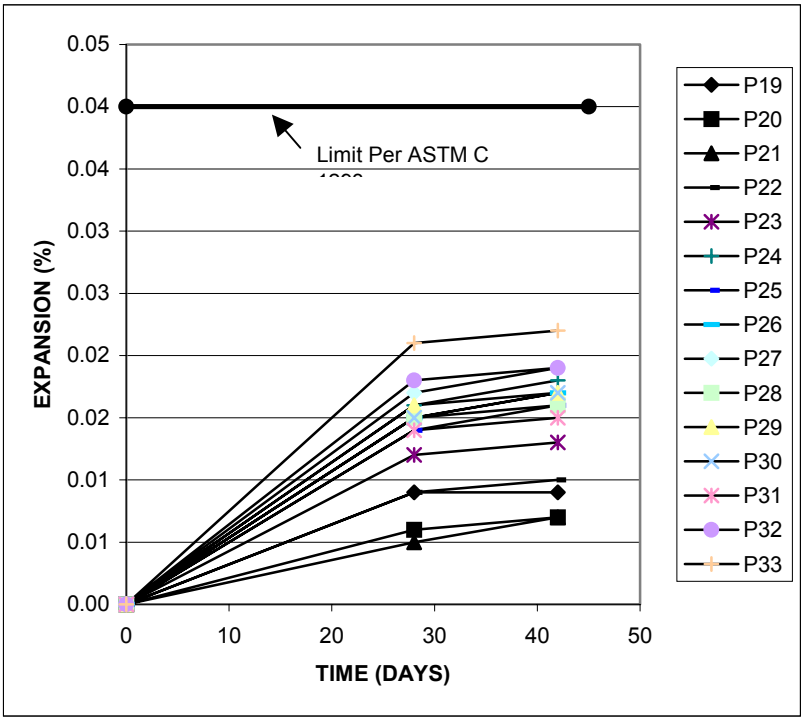

Figure 3.2 Expansion of Prisms 19 to 33, Moist Cured for 42 days at 23 °C

3.2.2 Expansion Testing of Laboratory CC

Following the concrete prism expansion tests, all prisms were crushed and mixed to the reference gradation. Sufficient water was then added to the crushed concrete and the mixture was allowed to sit in closed buckets for 24 hours to bring it to the 10% recommended moisture content before being compacted in a mold measuring 15.2 cm in diameter and 11.7 cm high. An average dry density of 1,954 kg/m^3 was achieved after application of the recommended compaction energy of 111,776 m-kg/m^3.

To measure expansion due to ASR attack, compacted CC samples were placed in both water and 1N-NaOH solution. All of the samples were then stored in a 38°C reaction-accelerating control chamber and allowed to expand. The test apparatus used to measure expansion of compacted CC is shown in Figure 3.3. Figure 3.4 shows expansion results for compacted CC samples from prisms 1 to 18; half of the samples were placed in water

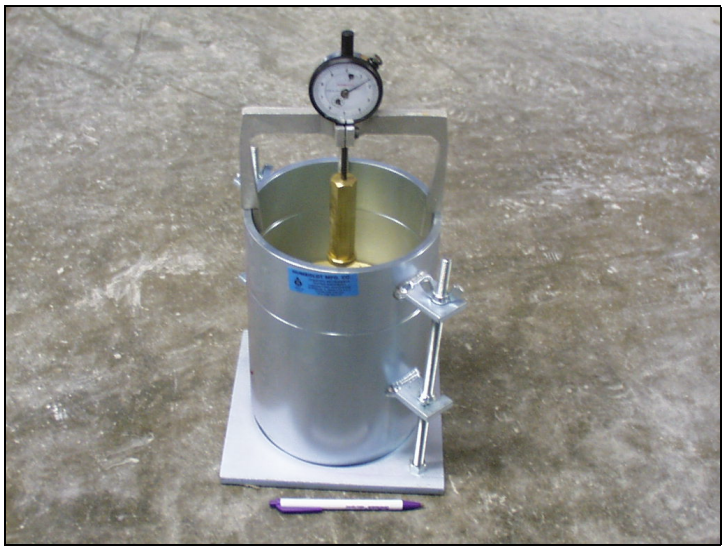

Figure 3.3 Test Apparatus for Compacted CC Expansion Samples

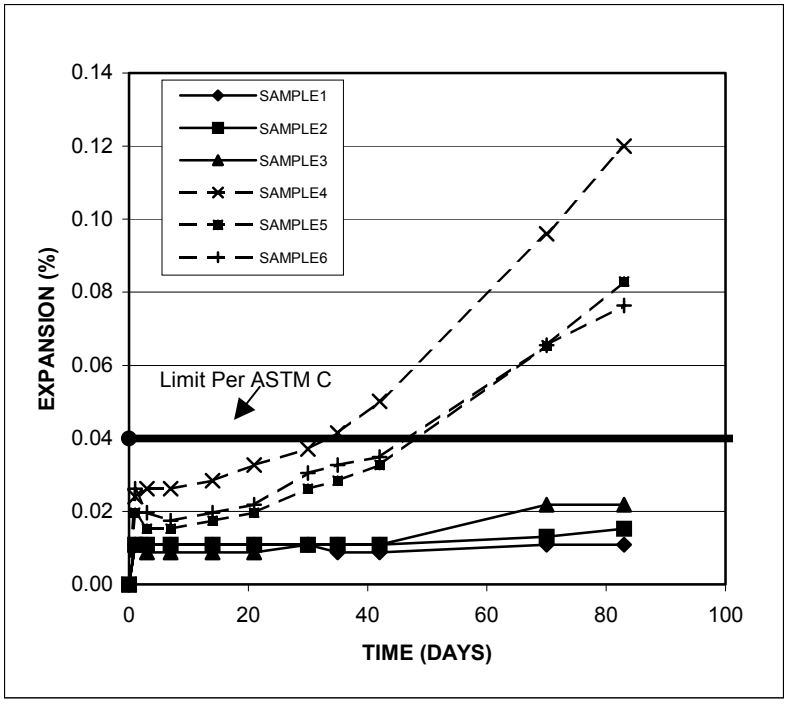

Figure 3.4 Compacted CC ASR Expansion Samples, Stored in 38°C Reaction Chamber. Samples 1,2,3 in Water; samples 4,5,6 in 1N-NaOH Solution (Samples 1-6 Prepared from Prisms 1 to 18, which that had Previously Experienced ASR Attack)

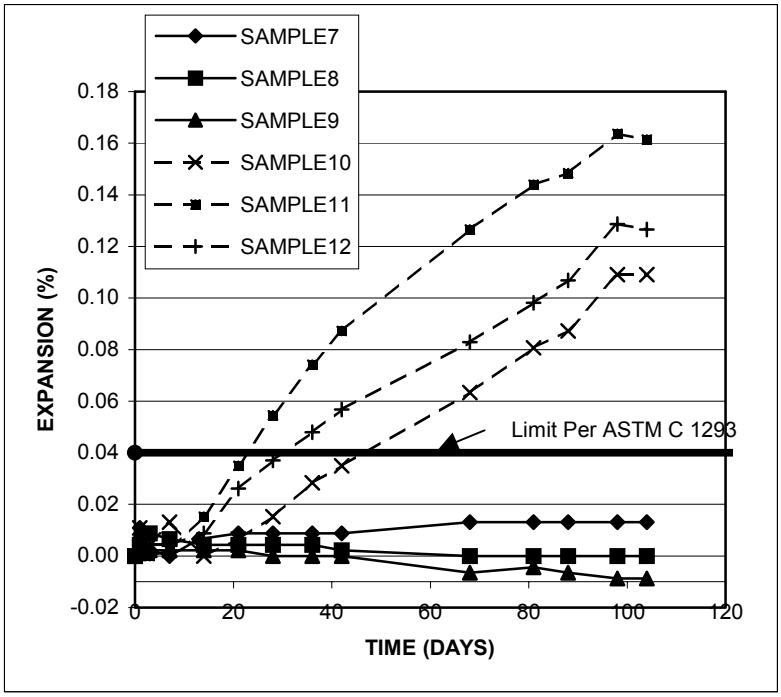

Figure 3.5 Compacted CC ASR Expansion Samples, Stored in 38 °C Reaction Chamber. Samples 7,8,9 in Water; Samples 10,11,12 in 1N-NaOH Solution (Samples 7-12 Prepared from Prisms 19 to 33 that had not Experienced ASR Attack)

(sample 1, 2, and 3) and half in 1N-NaOH solution (sample 4, 5, and 6). Likewise, Figure 3.5 shows compacted CC samples from prisms 19 to 33; half of the samples were placed in water (sample 7, 8, and 9) and half in 1N-NaOH solution (sample 10, 11, and 12). Placing the samples in water allowed for comparing the results with samples placed in the alkaline solution.

A limit of 0.04% expansion was used to indicate potential for ASR problems in concrete prisms. Although this expansion limit is reasonable for concrete, it is significantly low for compacted CC because there is no concern for structural cracking. Only excessive movements of the ground surface or facing panels are of concern in MSE walls. Because no limits have been established to characterize potential ASR problems in compacted crushed concrete, the 0.04% expansion has been used for discussions in ensuing sections.

3.2.3 Experimental Results and Discussions

In total, twelve molds were used to test expansion of compacted CC due to ASR attack. Expansion results of samples 1 to 6 can be seen in Figure 3.4. These are the crushed

and compacted concrete samples that were prepared from prisms 1 to 18, which were previously exposed to ASR attack in the 60°C control chamber.

The samples stored in water (samples 1, 2, and 3) did not experience any expansion and were below the 0.04% limit. The apparent explanation for this is that the alkalies in the CC were leached into the water, thus minimizing the effects of alkali aggregate reaction. IN contrast, samples 4, 5, and 6, which were stored in alkaline solution, continued to expand and reached an average maximum of 0.095% at around 80 days.

Test samples 7 to 12 were from concrete prisms moist cured at 23 °C. Unlike the first six, these samples had not been exposed to ASR expansion environment. Data in Figure 3.5 show that samples 7, 8, and 9, stored in water, did not expand and behaved in a similar manner to samples 1, 2, and 3 (Figure 3.4). Again, lack of expansion in compacted samples stored in water likely results from leaching of alkalis in the compacted CC. Therefore, alkalis were not available to react with the silica in the fine aggregates. Samples 10, 11, and 12, stored in alkaline solution, experienced an expansion much higher than the 0.04% limit with an average maximum expansion of 0.132% observed after 104 days (Figure 3.5).

The test results described provide important information about compacted CC composed of reactive aggregates. First, CC that has been previously exposed to ASR attack may continue to experience ASR reactions and expansion when exposed to a strong alkaline solution (Figure 3.4 - samples 4, 5, and 6). Second, when these samples are placed in a nonalkaline environment (as would be expected in free-draining backfill), they will not experience expansion due to ASR attack (Figure 3.4 - samples 1, 2, and 3). A similar conclusion can be inferred for samples that contained reactive aggregates but had not previously encountered ASR attack (Figure 3.5).

3.2.4 Expansion Testing of Commercial CC

An average compaction density of 2,002 kg/m^3 was achieved for three commercial CC specimens exposed to alkaline solution. It was not necessary to store samples in water, since previous results already showed that expansion due to ASR attack would not be experienced in this environment.

Expansion data on compacted CC samples from a commercial producer, stored in a 38°C reaction-accelerating chamber, are given in Figure 3.6. It can be observed from the

figure that the CC stored in alkaline solution did not expand to levels above the 0.04% limit. On the contrary, the samples tended to remain at essentially the same volume over the 57 days of exposure. These results suggest the absence of reactive aggregates in commercial crushed concrete. The laboratory CC samples stored in alkaline solution, on the other hand, exceeded the expansion limit, likely due to the presence of reactive aggregates in the crushed concrete.

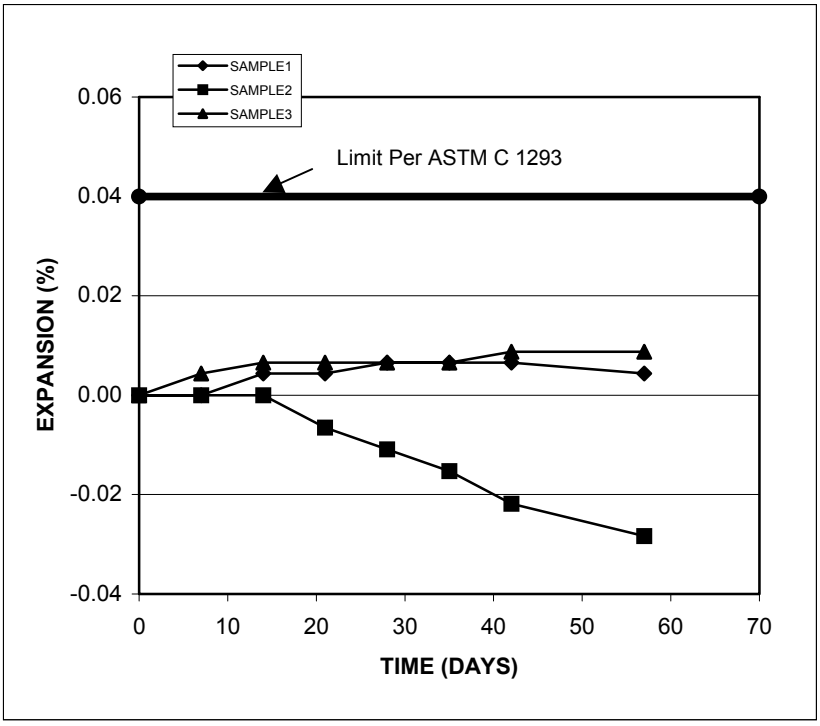

Figure 3.6 Compacted Commercial CC ASR Expansion Samples, Stored in 38 °C Reaction Chamber, in 1N-NaOH Solution

3.3 Sulfate Attack Testing Using Crushed Concrete

ASTM C 1012 is a standard test method for determining length change of hydraulic-cement mortars when exposed to sulfate solution. This test method was used as a guide to proportion the concrete mixture needed to prepare prisms for sulfate testing. Also, an expansion limit of 0.1% is proposed for use in ASTM C 1012 for mortar bar expansion using Type-V sulfate resistant cement. This limit was used in the evaluation of compacted crushed concrete exposed to sulfate attack.

ACI 211 (1991) absolute volume design procedure was used for proportioning the sulfate concrete mixture. A cement content of 244 kg/m^3 and a w/c ratio of 0.68 were used in this case. ASTM Type-1 cement, containing 4.2 mass % of SO_3, was the main binder in the concrete mixture. ASTM C 452 (a standard used for determining potential for expansion of Portland-Cement mortars exposed to sulfate) was utilized to calculate the amount of sulfate (mass % of SO_3) required for the concrete prism expansion test. Although a value of 7.0 mass % of SO_3 is specified in the standard, it was decided to boost this to 9% by adding gypsum to ensure expansion of concrete prisms above the specified limit of 0.1%. Table 3.3 shows the concrete mixture proportions for the sulfate test prisms.

Table 3.3 Sulfate Concrete Mixture Proportions (per m^3 of concrete) W/C=0.68, ACI 211

Materials	kg	BSG* (SSD)	AC**(OD)	Remarks
Cement	244	3.15	NA	ASTM Type-1 Cement
Gypsum	32	-	-	ASTM C 452
Water	166	1	NA	
Coarse Aggregate	896	2.62	0.8	ASTM C 33
Fine Aggregate	434	2.64	0.8	ASTM C 33
Calculation for Amount of SO_3 % Needed for Concrete Mixture, ASTM C 452				
ASTM Type-1 Cement SO_3% = 4.2 GYPSUM SO_3% = 45.2				
Percentage of cement and gypsum required to provide a mixture containing 9.0 mass % SO_3: Cement, % =((45.2 - 9)/(45.2 - 4.2))x100 = 88.3 Gypsum, % =((9 - 4.2)/(45.2 - 4.2))x100 = 11.7				
Amount of cement 244kg/m^3 (88.3%) Amount of gypsum needed (11.7 / 88.3)x244 =32 kg/m^3				

*BSG = Bulk Specific Gravity
**AC = Absorption Capacity

After mixing, the wet concrete was poured into thirty-six 7.6 by 7.6 by 25.4 cm steel mold prisms and three 10.2 by 20.4 cm cylinders and then consolidated to ensure uniform consistency. After curing for a day, the samples were unmolded and moist cured at 23°C. The prisms were then used for sulfate expansion tests while the cylinders were tested for compressive strength at different time intervals.

ASTM C1012 requires that mortar bars reach a compressive strength above 19,650 kPa (2850 psi) before being exposed to sulfate solution. Compressive strength test results

for three 10.2 by 20.4 cm concrete cylinders produced an average 29-day strength of 17,782 kPa (2580 psi), which was lower than that specified. This lower strength resulted from the fact that a high w/c ratio of 0.68 was used to ensure that expansion above 0.1% was achieved.

3.3.1 Accelerated Sulfate Expansion Tests

The thirty-six concrete prisms were divided into two groups. One set of prisms (1 to 18) was moist cured before being subjected to the ASTM C 1012 accelerated sulfate prism expansion test, at an elevated temperature of 38ºC and a standard sulfate exposure solution of 50,000 mg/L, 5% Na_2SO_4 solution. The intention here was to expose this group of prisms to expansion levels above the 0.1% limit. Prisms that had already been exposed to considerable sulfate attack would then used to produce laboratory recycled CC. To compare expansion of compacted crushed concrete from prisms already exposed to large chemical attack with that from prisms that had not been exposed to attack, a second set of prisms (19 to 36) was prepared. These were placed in saturated lime solution at 38°C until the accelerated expansion test on the first set of sulfate prisms (1 to 18) was completed.

After the expansion observation was stopped for prisms 1 to 18 (0.14% expansion at 30 days, Figure 3.7), the lengths of prisms 19 to 36 were measured and the expansion calculated from the initial length dimension. An average expansion of 0.13% at 30 days was observed for prisms 19 to 36 (Figure 3.8). This expansion exceeded the 0.1% limit and was also close to the 0.14% expansion measured for prisms 1 to 18. For this reason, only prisms 1 to 18 were used to prepare compacted crushed concrete. There was no need to use both sets because of the closeness of the prism expansion results. Obviously, the presence of high amounts of sulfate in the initial materials in the mixture (i.e., 9% SO_3) was sufficient to cause substantial expansion, irrespective of whether the prisms were stored in water or sulfate solution.

3.3.2 Expansion Testing of Laboratory CC

After preparing the sulfate samples to reference gradation, sufficient water was added to the crushed concrete and allowed to sit for 24 hours to bring it to the recommended moisture content of 10%, before compaction in a mold measuring 15.2 cm in diameter and

11.7 cm high. An average density of 2,050 kg/m^3 was achieved after the application of the recommended compaction energy of 111,776 m-kg/m^3.

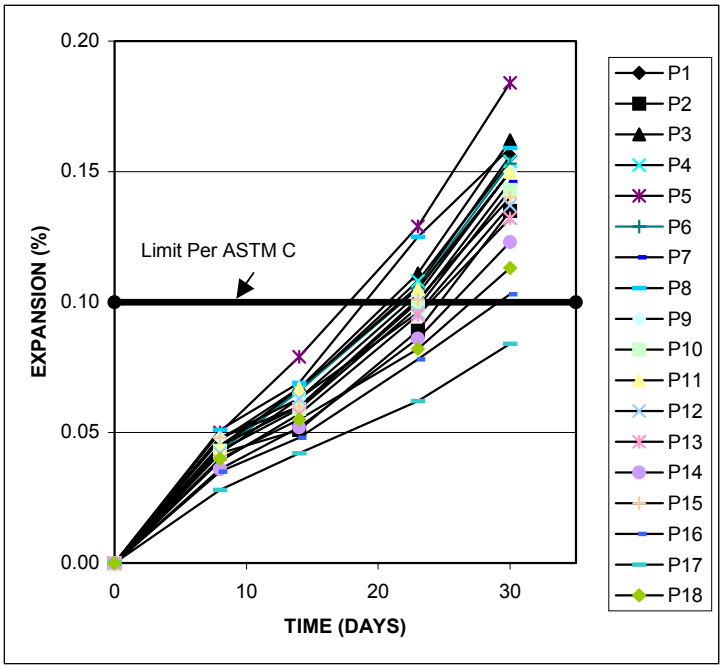

Figure 3.7 Expansion Prisms 1 to 18, Exposed to Sulfate Solution for 30 days, Stored in 38 °C Control Chamber

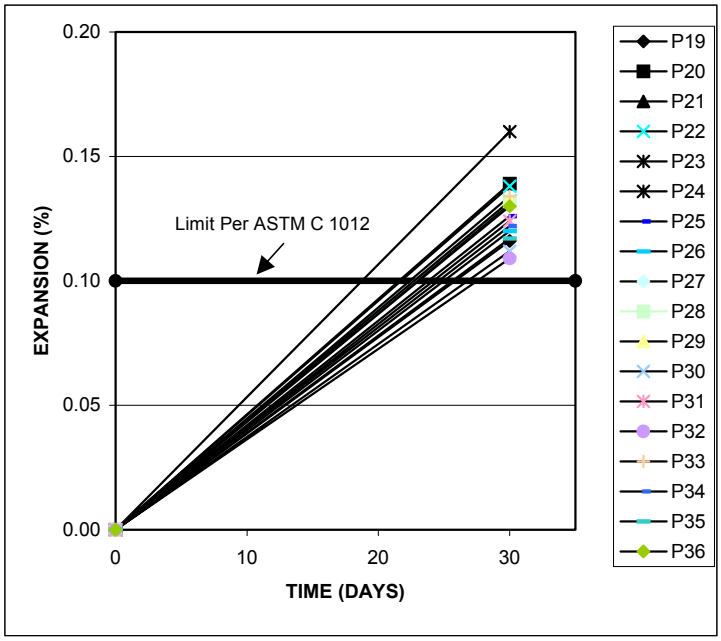

Figure 3.8 Expansion Prisms 19 to 36, Exposed to Saturated Lime Solution for 30 days, Stored in 38 °C Control Chamber

To measure expansion due to sulfate attack, compacted CC was placed in both water and 5% sulfate solution in a 38°C chamber. Figure 3.9 shows expansion results of compacted CC samples from prisms 1 to 18; half were placed in water (samples 1, 2, and 3) and half in sulfate solution (samples 4, 5, and 6). A limit of 0.1% expansion was used to indicate potential for sulfate problems in concrete prisms. Since no limits have been established to characterize potential sulfate problems in compacted crushed concrete used for MSE walls, the 0.1% expansion limit has been used for discussions relating to laboratory tests on compacted crushed concrete.

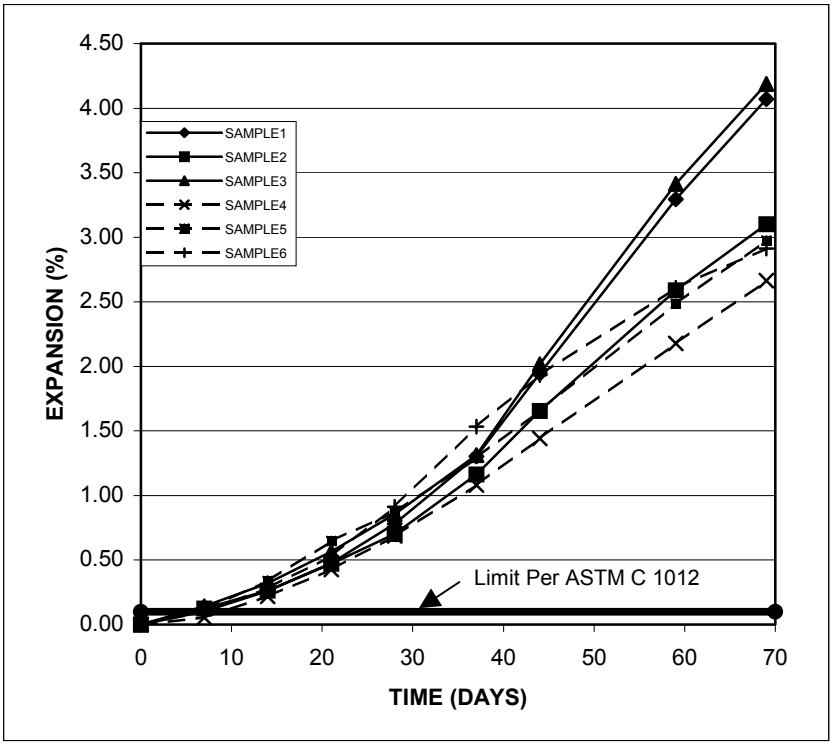

Figure 3.9 Compacted CC Sulfate Expansion Results, 38 °C Reaction Chamber. Samples 1,2,3 in Water; Samples 4,5,6 in 5% Sulfate Solution (Samples 1-6 Prepared from Prisms 1 to 18 that had Previously Experience Sulfate Attack)

3.3.3 Experimental Results and Discussions

In total, six molds were used to test expansion of compacted CC due to sulfate attack. Expansion results from samples 1 to 6 are shown in Figure 3.9. The samples stored in water (i.e., 1, 2, and 3) show an average expansion of 3.79% at 69 days. For those stored in sulfate solution, the average expansion was 2.85% at 69 days. The large expansions observed for the two cases result from the quantity of gypsum added to the concrete, resulting in a total of 9.0 %SO_3 by mass of cement and gypsum.

These results show that concrete that has previously experienced sulfate attack will continue to expand after crushing and compaction when exposed to very strong sulfate environment. In actual field practice, backfill will generally not contain concentrations of sulfate as high as those used in the lab. Also, tests on samples from the commercial producer reveal that only a small quantity of total sulfate was present in the CC (about

0.38%). Consequently, such large expansions, as those seen in the lab, should not be experienced in the field.

3.3.4 Sulfate Attack Testing of Commercial CC

After preparing commercial crushed concrete to the reference gradation and 10% moisture content, the material was compacted in molds and then exposed to the reaction solution. An average compaction density of 2,034 kg/m^3 was achieved for three samples exposed to sulfate solution.

Expansion of the compacted samples from a commercial producer, stored in 38°C in a reaction-accelerating chamber, is plotted in Figure 3.10. It was observed that the compacted CC, stored in 5% sulfate solution, expanded to levels more than 0.1% after 57 days of exposure. These results suggest that sufficient amounts of calcium hydroxide and monosulfate hydrate were still available for sulfate attack. Again, it should be noted that the exposure to 5% sulfate solution is very aggressive and not typical in actual MSE wall applications.

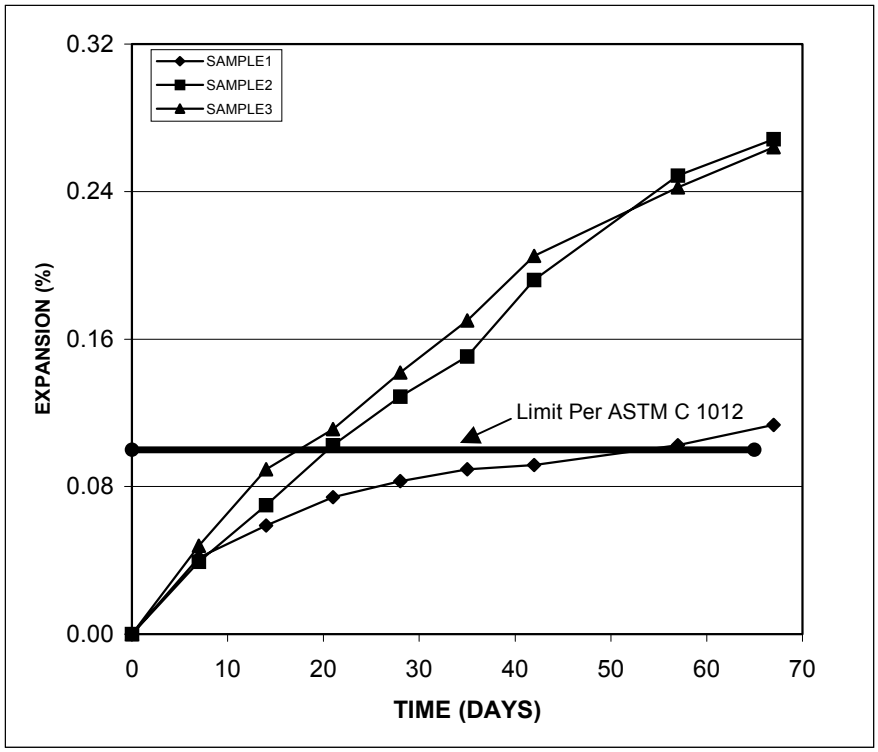

FIGURE 3.10 Compacted Commercial CC Sulfate Expansion, 38 °C Reaction Chamber, in 5% Sulfate Solution

3.4 Summary

ASR

Tests on samples prepared from laboratory-mixed concrete suggest that compacted CC may be subject to ASR attack when reactive aggregates are present in the mixture and when a strong alkaline environment is present (Figures 3.4 and 3.5).

However, commercially recycled CC is produced from pavements and structures that have had long periods of concrete hydration. In addition, CC may be stockpiled for many weeks before being transported to the backfill site. During its storage, alkalis in concrete may be leached out by atmospheric rainfall, thus resulting in reduced amounts of alkalis available to chemically react with siliceous aggregates. This deduction is supported by the results of high-silica lab CC samples placed in water (Figures 3.4 and 3.5), which did not experience any expansion over the period for which they were tested.

Also, expansion test results for commercial CC samples stored in 1N-NaOH alkali solutions, as shown in Figure 3.6, indicate that the material does not have sufficient amounts of reactive aggregates to result in ASR attack. An explanation for the lack of expansion is that materials used to manufacture recycled CC are generally obtained from many sources. For this reason, the likelihood of significant concentrations of large amounts of reactive aggregates is reduced. In contrast, compacted lab CC samples that yielded expansion greater than 0.04% (ASTM C 1293) were prepared using a concrete mixture with a very high alkali content (1.25% NaOH) and very reactive sand. These combinations may not be encountered in actual field practice.

Finally, information on seasonal precipitation-weighted mean concentrations from the National Atmospheric Deposition Program reveals that the pH of precipitation in Texas is approximately 5, which is more acidic than basic and will thus not contribute to ASR attack.

Sulfate Attack

Sulfate expansion results suggest that CC prepared from concrete that had previously experienced extensive sulfate attack may continue to expand after crushing and compaction. Because commercially produced CC is obtained from many different sources,

it is not expected that sulfate concentrations as great as those in the laboratory-prepared concrete (containing 9.0% SO_3 by mass) will be encountered in the field. Consequently, expansions related to sulfate attack in the actual backfill are not expected to be higher than those observed in the lab. Sulfate test results support the preceding conclusion, since at 60 days lab samples had an expansion above 2% (Figure 3.9) while that for commercial CC was below 0.32% (Figure 3.10).

It is interesting that commercially recycled CC specimens expanded to levels above 0.1% (ASTM C 1012) on exposure to 5% sulfate solution. This expansion implies that, although recycled CC has had a long time for hydration of cement to take place, sufficient amounts of calcium hydroxide were still available for sulfate attack.

Because MSE walls are usually constructed above the water table, sulfates from soil and groundwater should not be a major concern. But if large concentrations of sulfates are present in the rainwater, which percolates through the backfill material, sulfate attack may occur. Records of Texas precipitation show that sulfate concentrations of 1.215 mg/L are rather small compared with concentrations above 150 mg/L (ACI Building Code 318-83) that have been observed to cause sulfate attack. It is therefore unlikely that sulfate attack will affect CC used for MSE wall backfill.

4. Preliminary Results from Corrosion Studies

The use of recycled materials can be beneficial if these materials do not adversely affect the durability of a constructed MSE wall. Because these materials are often readily available on construction sites, using these recycled materials on the construction site where they are generated can result in reduced transportation and material costs. Research is thus being performed to determine the influence of crushed concrete (CC) and recycled asphalt pavement (RAP) on the corrosion performance of MSE wall reinforcing strips. This corrosion performance data will be used to estimate and compare service-life times of MSE walls backfilled with these recycled materials with those of MSE walls backfilled with conventional fill material (CFM). Because of the potential cost savings from using these recycled materials, a life-cycle cost analysis will be performed for MSE walls with different types of reinforcing strips and backfill materials under severe (chloride containing) and moderate (no chlorides) exposure conditions.

The following sections provide a brief description of the corrosion program being performed at Texas A&M University under project TxDOT 4177. The research is on schedule and is anticipated to be completed by the end of August 2003.

4.1 Materials

4.1.1 Aggregate

Three backfill materials, CFM, CC, and RAP, are under investigation to determine their effect on the corrosion of metallic reinforcing strips for MSE walls. Approximately 1.5 cubic yards of each type of backfill material was obtained from separate stockpiles at the Pickle Research Center in Austin, Texas. The materials were then transported to the Texas Transportation Institute in College Station, Texas. The Pickle Research Center obtained these backfill materials from the suppliers shown in Table 4.1.

Table 4.1 Selected sources of CFM, CC, and RAP backfill materials.

Material ID	Supplier	Location of Supplier
CFM	Texas Crushed Stone	Georgetown, Texas
CC	Big City Crushed Concrete	Dallas, Texas
RAP	TxDOT	Corpus Christi District, Texas

To maintain consistency among the research teams and eliminate the effect of particle size distribution in the comparison of the backfill materials, a reference gradation was proposed. By using the reference gradation, the differences between the backfill materials can be attributed to the backfill composition. The reference gradation that was followed is shown in Table 4.2.

To obtain the specified gradation for each material, each material was sieved on a mechanical shaker. The particle sizes were weighed and blended together for each material to attain the reference gradation.

Table 4.2 Reference gradation for CFM, CC, and RAP backfill materials.

Sieve No.	Diameter (mm)	Percent Passing
2”	50	100.0
1”	25	88.0
3/4”	12.5	65.0
4	4.75	35.0
8	2.36	22.0
16	1.18	15.0
40	0.43	7.0
100	0.15	1.5
200	0.08	0

Further characterization (i.e., pH, resistivity, chloride concentration, and redox potential, etc.) of the backfill materials has not yet been performed. Materials have been graded and are ready for each test.

4.1.2 Reinforcement

Ribbed galvanized-steel and plain-steel earth reinforcing strips were obtained from the Reinforced Earth Company for use on the project. The reinforcement received in the lab had approximate dimensions of 3/16 in by 1-7/8 in by 78 inches. These samples were then cut into smaller pieces using a band saw so that they could be embedded in the backfill materials for corrosion testing. The sample ends were ground to prevent potential sites of localized corrosion. The chemistry of the steel strips is currently being analyzed and data will be available on these compositions in the next report.

4.2 Experimental Design and Test Procedures

The experimental design consists of three main phases, as-received characterization of materials, short-term testing, and long-term testing. The as-received characterization testing was discussed in Rathje et al. (2001). The short-term testing was developed to examine the influence of the solution from the backfill materials on the corrosion of the reinforcing strips. The long-term testing will examine the corrosion of the earth reinforcing strips embedded within each backfill material.

4.2.1 Short-Term Test Procedures

Short-term testing requires that a solution be decanted from each of the backfill materials and used as an electrolyte in a corrosion cell to test the corrosion of the reinforcement. The testing is an attempt to provide results on how pore water from the backfill materials will impact the corrosion process. Three variables for the short-term experimental design have been identified; backfill type (CFM, CC, RAP), reinforcement type (galvanized-steel, G, or steel, S), and the presence of chlorides (no chlorides, NCl, or chlorides, Cl). Figure 4.1 shows the variables involved in the short-term testing.

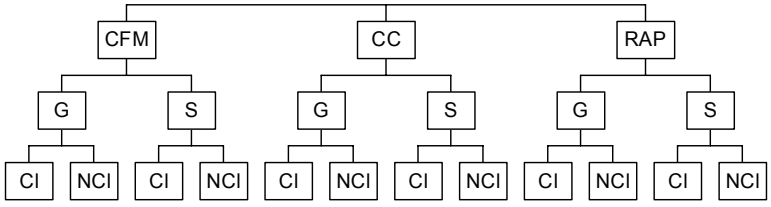

Figure 4.1 Short-term testing diagram.

The entire setup for this testing is complete. The research team needs eight more corrosion cells to start this testing. These have been ordered and delivery is anticipated by mid-November 2002. Testing will begin upon receiving the corrosion cells.

4.2.2 Long-Term Test Procedures

The long-term testing consists of embedding the reinforcement within each backfill material and monitoring the corrosion rate and potential. Four variables for the testing have been identified for the test program: backfill type (CFM, CC, RAP), reinforcement type

(galvanized-steel, G, or steel, S), presence of chlorides (no chlorides, NCl, or chlorides, Cl), and time of exposure (6 or 12 months). The program is shown in Figure 4.2. Eight samples are being evaluated for each combination of variables for a total of 96 samples. Figures 4.3 and 4.4 show the long-term corrosion samples.

Long-term testing is currently in progress. Fabrication of the long-term samples is complete and testing is in progress. Figure 4.3 shows the main components of a long-term test sample. Preliminary results from the testing program are discussed next.

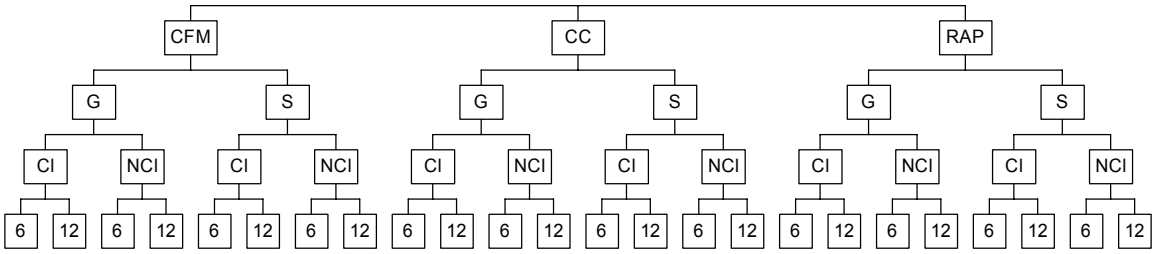

Figure 4.2 Long-term testing diagram.

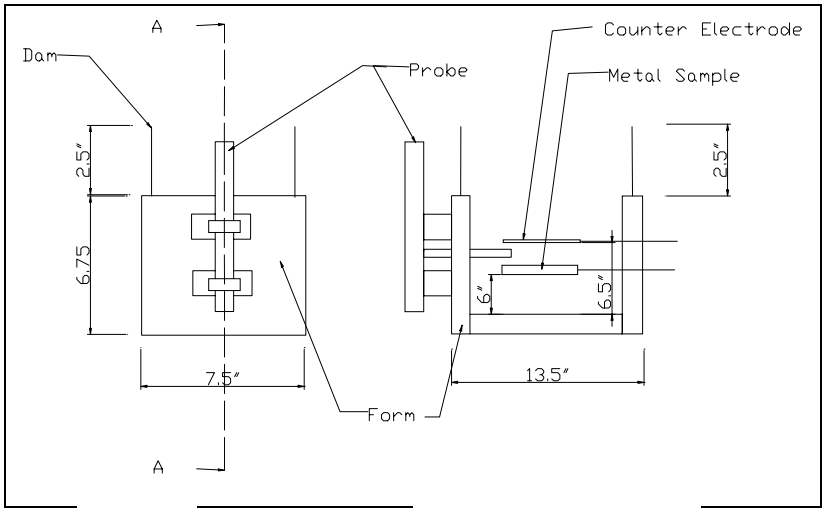

Front Side Section A-A

Figure 4.3 Front and sectional side view of long-term test samples equipped for polarization resistance testing.

4.3 Preliminary Results and Discussion

Two types of data are being collected from the corrosion samples; open circuit potential measurements and corrosion rates. These data are used to determine the likelihood of corrosion activity (potential) and the rate at which the metallic strips are corroding. It is anticipated that these data will be used to predict the time-to-corrosion and the time-to-failure, where failure is defined as the point where the strip has lost sufficient cross section and will no longer provide sufficient bond to the surrounding soil. For this study, the sum of the time-to-corrosion and time-to-failure is defined as the service-life. Because the objective of this study is to determine the influence of recycled materials on the corrosion of metallic strips used in MSE walls, service-life periods for the different systems (i.e., different backfill materials) will be determined and compared. A longer service-life would suggest a system that is more resistant to corrosion. However, because there may be potential cost savings from using recycled materials from the construction site, an economic analysis will be performed to determine the cost-effectiveness of the different systems under several scenarios. Service-life and life-cycle costing models are currently being developed while testing proceeds.

Potential readings and polarization resistance testing (corrosion rate testing) are being performed at regular time intervals. To determine the average corrosion rate for the different samples, the corrosion rates are being weighted based on the time of exposure between measurements. Figure 4.4 shows the results from averaging the corrosion rate data over a 64-day exposure period. Each boxplot represents two average values for each group. The line on the box represents the mean of the two points in this case. The samples are identified as follows: by backfill material type (CC, CFM, or RAP), metallic strip type (G or S), and exposure condition (Cl or NCl). Preliminary results from Figure 4.4 indicate that the metallic strips embedded in CFM may exhibit higher corrosion rates than metallic strips embedded in CC and RAP.

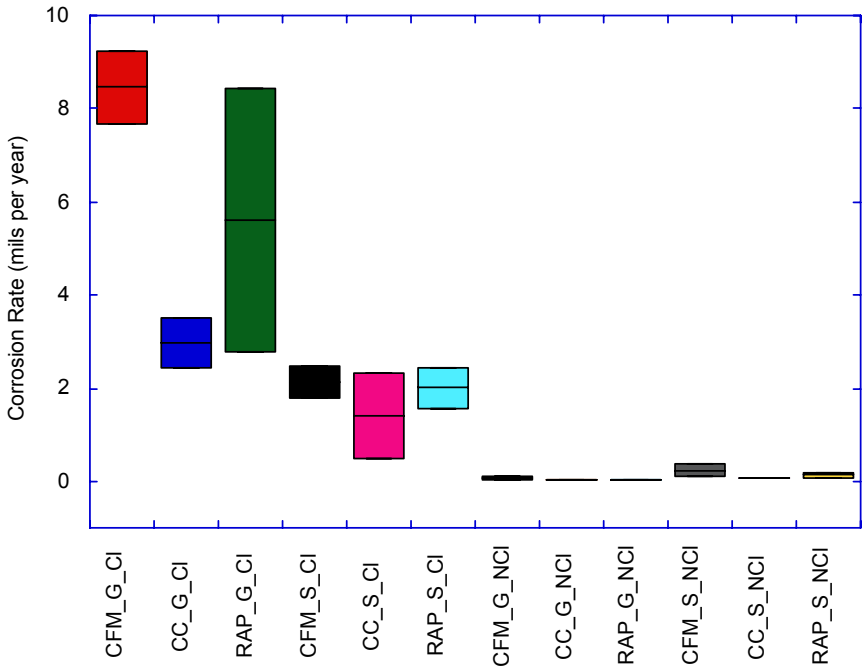

Figure 4.4 Boxplot of average corrosion rates for each group over 64 days.

However, to better compare the corrosion rates, a statistical analysis was performed on the corrosion rate data. At a 5% significance level, when only the backfill materials are compared, there is no significant difference in corrosion rates at this stage in the research project. However, when the corrosion rates from the different metallic strip types (galvanized steel or steel) are compared, the analysis indicates that at early exposure periods (up to 64 days) there is a significant difference. In addition, there is a significant difference between the mean corrosion rates when the environments (non-chloride or chloride) are compared, as revealed in Figure 4.4. All samples with no chloride exposure have average corrosion rates below 1 MPY, while those with chloride exposure are higher. These data represent only the first 64 days of testing. Therefore, final conclusions cannot yet be drawn from the data regarding the effectiveness of one backfill material over another.

In addition to corrosion rate data, testing is being performed to determine the open circuit potential readings as a function of time. As already noted, this information will be used to estimate the time-to-corrosion of metallic samples embedded in the different

backfill materials. The results from the potential readings are shown in Figure 4.4. Each group contains eight samples. The line in each box represents the median within the group. Open circuit potential values exhibiting more negative values in general indicate a higher likelihood of corrosion activation, although metallic type and environmental conditions can influence the absolute value of these readings. Note that in all cases shown in Figure 4.4, the open circuit potential is more negative for similar samples embedded in chloride (i.e., RAP_S_NCl compared with RAP_S_Cl, etc.). Because the corrosion rate data indicate that all samples exposed to chlorides are actively corroding and all samples exposed to the solution without chlorides are passive (no active corrosion), the potential where the sample passes from a passive state to an active state can be estimated. This is important because open circuit potential (or half-cell potential) readings are much easier to evaluate in the field.

To date, no statistical analysis has been performed on the potential data. Even so, some preliminary trends can be observed from Figure 4.4. Note that the CC has a higher average potential than the other backfill materials when the environment contains no chlorides. Because open circuit potential values that are more positive could indicate a lower likelihood of corrosion, the CC pore solution may be providing a passivating film on the strip reinforcement as a result of the higher pH. However, these data represent only the first 64 days of testing. Therefore, no conclusion yet can be drawn regarding the quality of one backfill material over another based on the potential data.

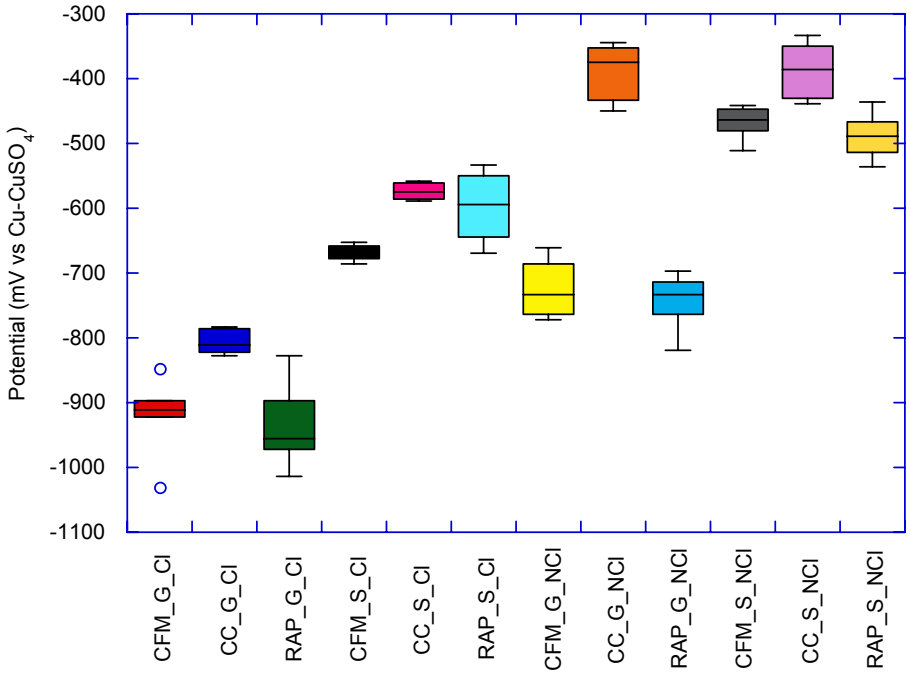

Figure 4.5 Boxplot of average potential readings for each group over 64 days.

4.4 Summary

Results indicate that the influence of recycled materials as backfill materials, specifically CC and RAP, do not adversely affect the corrosion rate of the metallic strip reinforcement at early exposure periods. Exposure of MSE wall strip reinforcement to chlorides significantly increases the corrosion rate of these materials at early exposure periods. In addition, at early exposure periods, galvanized strip reinforcement, especially when exposed to chloride environments, exhibits higher corrosion rates than conventional plain steel strip reinforcement.

5. Summary

MSE walls are common highway structures in Texas and throughout the United States. These earth-retaining structures are made up of facing panels, reinforcement elements, and high-quality granular backfill. In areas where high-quality granular backfill is not available, recycled materials such as RAP and CC may provide cost-effective alternatives.

This research report describes preliminary results from the various components of the project. A summary of pertinent results to date is given below.

Geotechnical - The geotechnical characterization of RAP and CC focused on evaluating potential material breakdown during compaction, assessing the accuracy of the nuclear gauge to measure the properties of the field-compacted materials, and triaxial strength testing. Compaction tests revealed that the percentage of fines increased most for the CFM (3.6%), while the increases for CC and RAP were much lower (1.6 and 0.6 %, respectively). Consequently, material breakdown does not appear to be a major concern for CC or RAP.

Field evaluation of as-compacted moist density and water content using the nuclear gauge and traditional methods indicated significant differences. Moist densities measured with the nuclear gauge were generally 10 to 20% larger than those measured with the rubber balloon method. Water contents measured with the nuclear gauge were consistently larger than those measured with oven drying. For CC the difference was modest (20%), but for RAP the nuclear gauge reported water content values three times as large as the oven-dry values. This error occurs because the nuclear gauge infers water content from the amount of hydrogen in the material, and RAP contains a significant amount of hydrogen in the asphalt binder. As a result of these findings, it is recommended that material-specific calibrations be developed on site when using the nuclear gauge for CC and RAP.

Triaxial compression testing was performed on CC, RAP, and CFM. The CC and CFM display excellent strength, with effective friction angles of about 55°. The RAP did not exhibit such large strength, with a friction angle of 39° and an effective cohesion of 8 psi. The smaller strength is attributed to the bitumen coating around the particles. Although

lower than the other materials, the strength of RAP is still adequate for MSE wall applications. Additional tests are underway to confirm these preliminary findings.

Finally, a large-scale direct shear device was designed and constructed to measure the shear strength of the full gradation of the test materials. This device was recently delivered and initial calibration tests are being performed. This device will be used for the shear strength and pull-out tests.

CC Durability – Expansion tests were performed on various crushed concrete specimens to evaluate the potential for excessive heave or expansion after compaction. To study the worst-case scenario, two mixes of laboratory concrete were made- one prone to alkali-silica reaction (ASR) and one prone to sulfate attack. CC specimens were constructed from each of these mixes, soaked in various agents, and the expansion was measured. For the ASR concrete, only minor expansion was observed when the CC was soaked in water. More noticeable expansion occurred when soaked in an alkaline solution. For the sulfate-rich concrete, up to 4% expansion was observed. This is a significant amount of the expansion that could damage an MSE wall. However, the sulfate concentration in the lab concrete was significantly larger than would be encountered in the field, and therefore, expansion in the field should be less. For comparison, the stockpiled CC used for the other phases of this project was also tested. These CC specimens displayed only minor expansion, if any.

Corrosion – Short-term and long-term corrosion tests are part of the planned corrosion studies. The short-term tests are set to begin in November 2002. The long-term corrosion tests are underway. These tests involve embedding reinforcement within each backfill material and monitoring the corrosion rate and potential. After 64 days of testing, the preliminary results indicate that the influence of recycled materials as backfill materials, specifically CC and RAP, do not adversely affect the corrosion rate of the metallic strip reinforcement at early exposure periods. Exposure of MSE wall strip reinforcement to chlorides significantly increases the corrosion rate of these materials at early exposure periods. In addition, at early exposure periods, galvanized strip reinforcement, especially when exposed to chloride environments, exhibits higher corrosion rates than conventional plain steel strip reinforcement.

References

ACI Committee 211 (1991). "Standard Practice for Selecting Proportions for Normal, Heavy-Weight and Mass Concrete," ACI 211.1 Report, American Concrete Institute Manual of Concrete Practice, Part 1.

ACI 318-02 (2002) *Building Code Requirements for Structural Concrete and Commentary*, American Concrete Institute, Farmington Hills, MI.

ASTM (2001). "Standard Test Method for Density, Relative Density (Specific Gravity), and Absorption of Coarse Aggregate (ASTM C127)." *Annual Book of ASTM Standards,* American Society for Testing and Materials, West Conshohocken, PA.

ASTM (2001). "Standard Test Method for Potential Expansion of Portland-Cement Mortars Exposed to Sulfate (ASTM C452)." *Annual Book of ASTM Standards,* American Society for Testing and Materials, West Conshohocken, PA.

ASTM (2001). "Standard Test Method for Length Change of Hydraulic-Cement Mortars Exposed to a Sulfate Solution (ASTM C1012)." *Annual Book of ASTM Standards,* American Society for Testing and Materials, West Conshohocken, PA.

ASTM (2001). "Standard Test Method for Determination of Length Change of Concrete Due to Alkali Silica Reaction (ASTM C1293)." *Annual Book of ASTM Standards,* American Society for Testing and Materials, West Conshohocken, PA.

ASTM (2001). "Standard Test Method for Particle-Size Analysis of Soils (ASTM D422)." *Annual Book of ASTM Standards,* American Society for Testing and Materials, West Conshohocken, PA.

ASTM (2001). "Standard Test Method for Specific Gravity of Soils (ASTM D854)." *Annual Book of ASTM Standards,* American Society for Testing and Materials, West Conshohocken, PA.

ASTM (2001). "Standard Specification for Reagent Water (ASTM D1193)." *Annual Book of ASTM Standards,* American Society for Testing and Materials, West Conshohocken, PA.

ASTM (2001). "Standard Test Methods for Density and Unit Weight of Soil in Place by the Sand-Cone Method (ASTM D1556)." *Annual Book of ASTM Standards,* American Society for Testing and Materials, West Conshohocken, PA.

ASTM (2001). "Standard Test Method for CBR of Laboratory-Compacted Soils (ASTM D1883)." *Annual Book of ASTM Standards,* American Society for Testing and Materials, West Conshohocken, PA.

ASTM (2001). "Standard Test Methods for Density and Unit Weight of Soil in Place by the Rubber Balloon Method (ASTM D2167)." *Annual Book of ASTM Standards*, American Society for Testing and Materials, West Conshohocken, PA.

ASTM (2001). "Standard Test Method for Permeability of Granular Soils (Constant Head) (ASTM D2434)." *Annual Book of ASTM Standards*, American Society for Testing and Materials, West Conshohocken, PA.

ASTM (2001). "Standard Test Methods for Density of Soil and Soil-Aggregate in Place by Nuclear Methods (Shallow Depth) (ASTM D2922)." *Annual Book of ASTM Standards*, American Society for Testing and Materials, West Conshohocken, PA.

ASTM (2001). "Standard Test Methods for Density of Bituminous Concrete in Place by Nuclear Methods (ASTM D2950)." *Annual Book of ASTM Standards,* American Society for Testing and Materials, West Conshohocken, PA.

ASTM (2001). "Standard Test Method for Direct Shear Test of Soils under Consolidated Drained Conditions (ASTM D3080)." *Annual Book of ASTM Standards,* American Society for Testing and Materials, West Conshohocken, PA.

ASTM (2001). "Standard Test Methods for Maximum Index Density and Unit Weight of Soils Using a Vibratory Table (ASTM D4253)." *Annual Book of ASTM Standards,* American Society for Testing and Materials, West Conshohocken, PA.

ASTM (2001). "Standard Test Methods for Minimum Index Density and Unit Weight of Soils and Calculation of Relative Density (ASTM D4254)." *Annual Book of ASTM Standards,* American Society for Testing and Materials, West Conshohocken, PA.

ASTM (2001). "Standard Test Methods for Density of Soil and Rock in Place by the Water Replacement Method in a Test Pit (ASTM D5030)." *Annual Book of ASTM Standards*, American Society for Testing and Materials, West Conshohocken, PA.

Black, K. N. (1995). "The Nuclear Asphalt Content Gauge." *Public Roads*, Winter, Vol. 58, No. 3, pp. 8-13.

Burati, J. L., and Elzoghbi, G. B. (1987). "Correlation of Nuclear Density Results with Core Densities." *Transportation Research Record*, Vol. 1126, Transportation Research Board, National Research Council, Washington, D.C., pp. 53-67.

Carter, M. and Bentley, S. P. (1991). *Correlations of Soil Properties*. Pentech Press, London.

Dent Glaser, L. S. and Kataoka, N. (1981). "The Chemistry of Alkali-Aggregate Reactions." Proceedings of the 5th International Conference on Alkali-Aggregate Reaction, Cape Town, S252/23.

Elias, V., and Christopher, B. (1996). "Mechanically stabilized earth walls and reinforced soil slopes design and construction guidelines." FHWA Demonstration Project 82, *FHWA SA-96-071*.

Federal Highway Administration (FHWA) (2000). "User guidelines: Reclaimed asphalt pavement, reclaimed concrete material." http://www.tfhrc.gov//////hnr20/recycle/waste/, accessed October 1, 2000.

Jones, D. A. (1996) *Principles and Prevention of Corrosion*. Prentice Hall, Upper Saddle River, NJ.

Kelly, T. (1998). "Crushed Cement Concrete Substitution for Construction Aggregates – A Materials Flow Analysis," U.S. Geological Survey Circular.

Kennedy, T. W., Tahmoressi, M., and Solaimanian, M. (1989). "Evaluation of a Thin-Lift Nuclear Gauge." *Transportation Research Record*, Vol. 1217, Transportation Research Board, National Research Council, Washington, D.C., pp. 9-19.

Mamlouk, M. S. (1988). “Nuclear Density Testing of Granular Materials: State of the Art.” *Research Report No. FHWA-AZ88-839*, Federal Highway Administration.

Mehta, P. K., and Monteiro, J. M. (1993). *Concrete: Structure, Properties and Methods*. 2nd edition, Prentice Hall, Englewood Cliffs, N.J.

Mitchell, J.K. and Christopher, B. (1990). “North American Practice in Reinforced Soil Systems,” *Geotechnical Special Publication No. 25, Design and Performance of Earth Retaining Structures*, June 18-21, Ithaca, NY, pp. 322-346.

Morris, D. V., and Delphia, J. G. (1999). “Specifications for Backfill of Reinforced-Earth Retaining Walls.” *Texas Transportation Institute*, *FHWA/TX-99/1431-S*.

Nagi, M., and Whiting, D. (1999). “Evaluation of Precision of a Nuclear Gauge for Measurement of Water and Cement Content of Fresh Concrete.” *Cement, Concrete, and Aggregates*, CCAGDP, Vol. 21, No. 1, June 1999, pp. 1-11.

National Atmospheric Deposition Program, (2002). “Seasonal Precipitation-Weighted Mean Concentrations.” http://nadp.sws.uiuc.edu/nadpdata/state.asp?state=TX, accessed May 18, 2002.

Rathje, E. M., Rauch, A. F., Folliard, K. J., Trejo, D., Little, D., Viyanant, C., Ogolla, M., and Esfeller, M. (2001). "Recycled Asphalt Pavement and Crushed Concrete Backfill: State-of-the-art review and Material Characterization." *Research Report* 0-4177-1, Texas Department of Transportation, Austin, Texas, October.

Regimand, A., and Gilbert, A. B. (1999). “Apparatus and Method for Field Calibration of Nuclear Surface Density Gauges.” *Field Instrumentation for Soil and Rock*, ASTM STP 1358, Eds., G. N. Durham and W. A. Marr, American Society for Testing and Materials, West Conshohocken, PA, pp. 135-147.

Sanders, S. R., Rath, D., and Parker Jr., F. (1994). “Comparison of Nuclear and Core Pavement Density Measurements.” *Journal of Transportation Engineering*, Vol. 120, Issue 6, pp. 953-966.

Skempton, A. W. (1954). “The Pore Pressure Coefficients A and B.” *Géotechnique,* Vol. 4, pp. 143-147.

Thaulow, N., and Jakobsen, U. H. (1995). “The Diagnosis of Chemical Deterioration of Concrete by Optical Microscopy,” *Mechanisms of Chemical Degradation of Cement-Based Systems*, Eds. K.L. Scrivener and J.F. Young, 1st edition, pp. 5-9

Taylor, H. F. W (1997). *Cement Chemistry*. 2nd edition, T. Telford, London, pp. 361-373.

Texas Department of Transportation (1993). Standard Specifications for Construction of Highways, Streets and Bridges. pp. 625-627.

Texas Department of Transportation, Tex-110-E (2001). *Particle Size Analysis of Soils*.

Texas Department of Transportation, Tex-113-E (2001). *Laboratory Compaction Characteristics and Moisture-Density Relationship of Base Materials*.

Texas Department of Transportation, Tex-114-E (2001) *Laboratory Compaction Characteristics and Moisture-Density Relationship of Subgrade and Embankment Soils*.

Texas Department of Transportation, Tex-400-A (2001). *Sampling Stone, Gravel, Sand, and Mineral Aggregates*.

Texas Department of Transportation, Tex-401-A (2001). *Sieve Analysis of Fine and Coarse Aggregate*.

Troxler Electronics, Inc. (2001). "Manual of Operation and Instruction: Model 3440 Surface Moisture-Density Gauge." Troxler Laboratories, Research Triangle Park, North Carolina, 220 pages.

U.S Department of Commerce, National Technical Information Services (1999). *Mechanically Stabilized Earth Walls and Reinforced Soil Slopes Design and Construction Guidelines, FHWA Demonstration Project 82, Reinforced Soil Structures MSEW and RSS*, pp. 57-74.